Energy spectrum of GaAs-AlGaAs Coupled Quantum Well

Shahriar Pollob, Sujaul Chowdhury*
Department of Physics, Shahjalal University of Science and Technology, Sylhet 3114, Bangladesh
*Email: s.chowdhury-phy@sust.edu *ORCID: https://orcid.org/0000-0001-6862-9989

ABSTRACT: We have calculated energy spectrum of electron in conduction band of GaAs-AlGaAs Coupled Quantum Well (CQW) consisting of two Quantum Wells (QW) of equal depth but unequal width. We find that confined energy levels of isolated QWs become quasi-bound energy levels of the CQW. Moreover, if confined energy levels of different quantum numbers of the two isolated QWs match in energy, we find that energy level of CQW becomes energy doublet. We first derived a transcendental equation (exact within conventional approximations) that is obeyed by the quasi-bound energy levels for electron in conduction band of GaAs-AlGaAs CQW and then obtained these results by numerical investigations of the equation.

Keywords: Coupled Quantum Well, quasi-bound energy levels, GaAs-AlGaAs, Nanostructure Physics, numerical investigation, root-finding, Mathematica

I. INTRODUCTION

GaAs-AlGaAs Coupled Quantum Well (CQW) is a very interesting semiconductor nanostructure [1-5]. Matter-wave associated with an electron residing in the CQW can feel both the Quantum Wells (QW) and the separating thin tunnel barrier at a time. An electron can tunnel the thin barrier easily and can dwell in the entire nanostructure. D. K. Ferry and S. M. Goodnick [1] summarized nanostructure Physics of CQW. They [1] demonstrated that in case of symmetric CQW having thin tunnel barrier, every quasi-bound energy level of CQW is a doublet. They [1] also showed that in case of asymmetric CQW, one can apply bias voltage with appropriate polarity to allow two energy levels of different quantum numbers of the two QWs to match in energy scale for energy levels to become doublet. They [1] mentioned that in symmetric case, energy levels of any given doublet can be calculated by degenerate perturbation theory [6]. S. Chowdhury and M. J. Iqbal [2] calculated energy spectrum of symmetric CQW using standard transfer matrix method instead, utilizing the information that eigenfunctions decay to zero sufficiently outside the region of CQW. S. Chowdhury and M. Rahman [3] explored non-tunneling regime of CQW; they calculated transmission probability of electron across GaAs-AlGaAs CQW as a function of energy in non-tunneling regime. U. K. Chowdhury and S. Chowdhury [4, 5] calculated effect of magnetic field applied normal to GaAs-AlGaAs interfaces of CQW on quasi-bound energy levels of CQW. W. L. Bloss [7] calculated effect of electric field on eigenstates of symmetric GaAs-AlGaAs CQW. B. Olejnikova [8] calculated effect of electric field on asymmetric CQW. There is a large number of recent works on CQW dealing with optical effects.

From reference [1] to [4], one may assume that CQW is now a textbook [1] problem. But our work in this paper shows that the story is far from complete. Confined energy levels of an isolated GaAs-AlGaAs QW depend on both depth and width of the QW [9, 10]. If two QWs of unequal width come close to form CQW, the energy spectrum that results remains an open question. In this paper we address this open issue. In this paper, we report energy spectra of GaAs-AlGaAs CQW consisting of two QWs of equal depth but unequal widths. Using transfer matrix method, we first derived an exact (within conventional approximations) transcendental equation obeyed by quasi-bound energy levels for electron in conduction band of the CQW. The equation reduces to that of reference [2] if the two QWs are equal in width also, i.e. for symmetric CQW. Our extensive numerical investigations presented in this paper have revealed surprising results that we could not fathom before.

II. CALCULATIONS

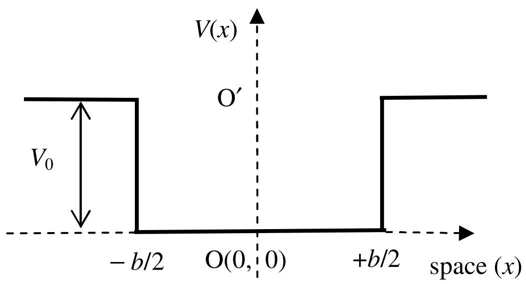

FIG 1. Showing potential energy profile for electron in conduction band of an isolated GaAs-AlGaAs QW

Using the potential energy profile shown in Figure 1, confined energy levels of isolated QW are found to obey the two transcendental equations [9, 11] given by equation (1) and (2).

$$\tan\left(\frac{b}{2}\sqrt{\frac{2mE}{\hbar^2}}\right)=\sqrt{\frac{V_0}{E}-1} \quad (1)$$

$$-\cot\left(\frac{b}{2}\sqrt{\frac{2mE}{\hbar^2}}\right)=\sqrt{\frac{V_0}{E}-1} \quad (2)$$

Here values of E are allowed values of kinetic energy of an electron for motion along x direction i.e. for motion normal to GaAs-AlGaAs interfaces of the QW; as such values of E are positive. If we take $(x, V) = (0 , 0)$ at O′ rather than O, see Figure 1, allowed values of E would be negative quantities. The positive values of E are less than V_0, which ensures that the electron cannot (classically) go out of QW and is essentially confined within the QW.

10.29322/IJSRP.15.11.2025.p16747

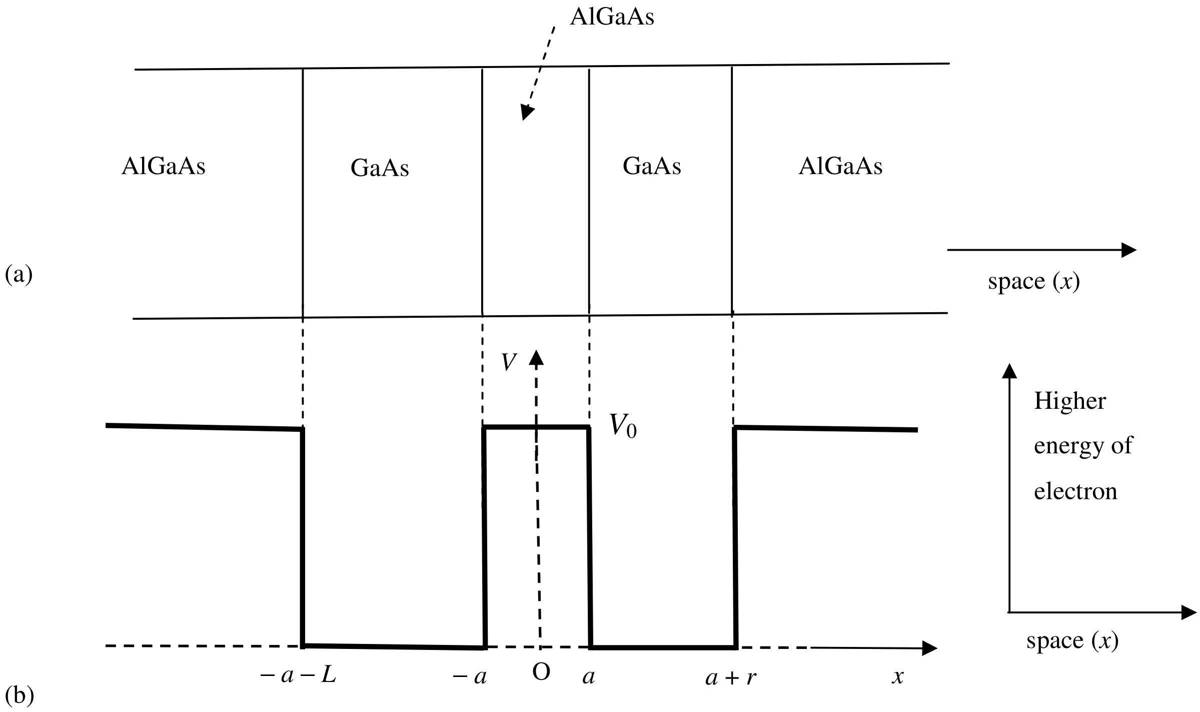

FIG 2. (a) Material structure (b) band model of GaAs-AlGaAs Coupled Quantum Well. O is origin (x, V) = (0, 0). Potential energy V is zero in the Quantum Wells because of the choice of origin. QW widths L and r are different.

Using the potential energy profile of Figure 2(b) which corresponds to material structure of CQW shown in Figure 2(a), we have derived the transcendental equation given by Equation (3) using transfer matrix method with the information that eigenfunctions decay to zero sufficiently outside the region of CQW.

$$\begin{aligned}&\left[4+\left(\frac{\alpha}{\beta}-\frac{\beta}{\alpha}\right)^2\right]\cos(\alpha(L-r))\\&+\left[4-\left(\frac{\alpha}{\beta}-\frac{\beta}{\alpha}\right)^2\right]\cos(\alpha(L+r))\\&-4\left(\frac{\alpha}{\beta}-\frac{\beta}{\alpha}\right)\sin(\alpha(L+r))\\&-\left(\frac{\alpha}{\beta}+\frac{\beta}{\alpha}\right)^2 e^{-\beta(4a)}\cos(\alpha(L-r))\\&+\left(\frac{\alpha}{\beta}+\frac{\beta}{\alpha}\right)^2 e^{-\beta(4a)}\cos(\alpha(L+r))\\&=0\end{aligned} \quad (3)$$

Here $\alpha^2 = \frac{2mE}{\hbar^2}$ and $\beta^2 = \frac{2m}{\hbar^2}(V_0 - E)$. Here $2a$ is width of the tunnel barrier separating the two QWs. L and r are widths of left and right hand QW respectively. V_0 is depth of the QWs as well as height of the tunnel barrier given by $773x$ meV where x is Al content of $Al_xGa_{1-x}As$. $m = 0.067m_e = 0.067\times9.1\times10^{-31}$ kg is effective mass of electron in conduction band of GaAs. See Figure 2. Here values of E are allowed values of kinetic energy of an electron in QW regions for motion along x direction i.e. for motion normal to GaAs-AlGaAs interfaces of the QWs; as such values of E are positive.

As to isolated GaAs-AlGaAs QW, we have graphically solved [9, 11] equation (1) and equation (2) and obtained allowed values of E. As to GaAs-AlGaAs CQW, we have obtained allowed values of E by numerically solving equation (3); we used root-finding method, so called bisection method [11], and obtained allowed values of E.

III. RESULTS

See Figure 3, TABLE I and TABLE II for the most striking result of our extensive numerical investigations. We find that confined energy levels of individual QW become allowed energy levels in the CQW. In other words, allowed values of energy of an electron in a given QW for motion normal to GaAs-AlGaAs interfaces become allowed values of energy of the electron in the CQW for motion normal to GaAs-AlGaAs interfaces.

10.29322/IJSRP.15.11.2025.p16747

TABLE I Energy spectrum of CQW. Well widths $L = 20$ nm, $r = 15$ nm, Al content of $Al_xGa_{1-x}As$ $x = 0.1$

$2a$ (nm)	E_1 (meV)	E_2 (meV)	E_3 (meV)	E_4 (meV)	E_5 (meV)
2	7.267	13.423	32.103	51.252	73.759
4	8.276	13.310	32.963	50.392	71.810
6	8.538	13.272	33.297	49.950	70.605
8	8.604	13.261	33.414	49.751	69.905
10	8.621	13.258	33.454	49.666	69.502

TABLE II Energy spectrum of isolated GaAs-$Al_xGa_{1-x}As$ QW for $x = 0.1$

QW width b (nm)	E_1 (meV)	E_2 (meV)	E_3 (meV)
15	13	50	
20	9	33	69

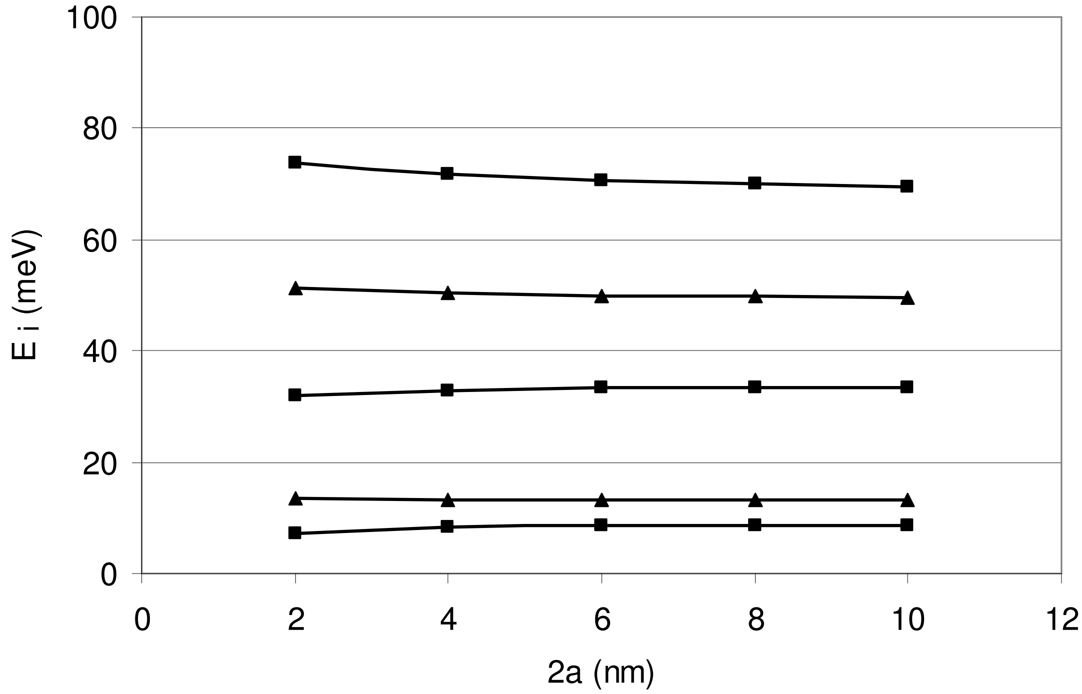

FIG 3. Quasi-bound energy levels of CQW for various widths $2a$ of tunnel barrier between the two QWs of widths $L = 20$ nm and $r = 15$ nm and depth $773x = 77.3$ meV for Al content $x = 0.1$ of $Al_xGa_{1-x}As$. Squares originate from isolated left hand QW and triangles originate from isolated right hand QW. See TABLE I and TABLE II for the data.

TABLE III Confined energy levels of isolated GaAs-AlGaAs QWs of depth 154.6 meV and widths 3.8 nm and 20 nm

QW width (nm)	E_1 (meV)	E_2 (meV)	E_3 (meV)	E_4 (meV)
3.8	86			
20	10	39	86	142

3

10.29322/IJSRP.15.11.2025.p16747

TABLE IV Quasi-bound energy levels of GaAs-AlGaAs CQW of depth 154.6 meV and width 20 nm for left hand QW and 3.8 nm for right hand QW separated by tunnel barrier of width $2a$.

$2a$ (nm)	E_1 (meV)	E_2 (meV)	E_3 (meV)	E_4 (meV)	E_5 (meV)
2	9.622	37.343	73.426	100.711	150.401
4	9.832	38.720	79.066	93.023	146.199
6	9.859	38.946	82.104	89.061	144.256
8	9.863	38.984	83.686	87.156	143.337
10	9.863	38.990	84.492	86.247	142.879

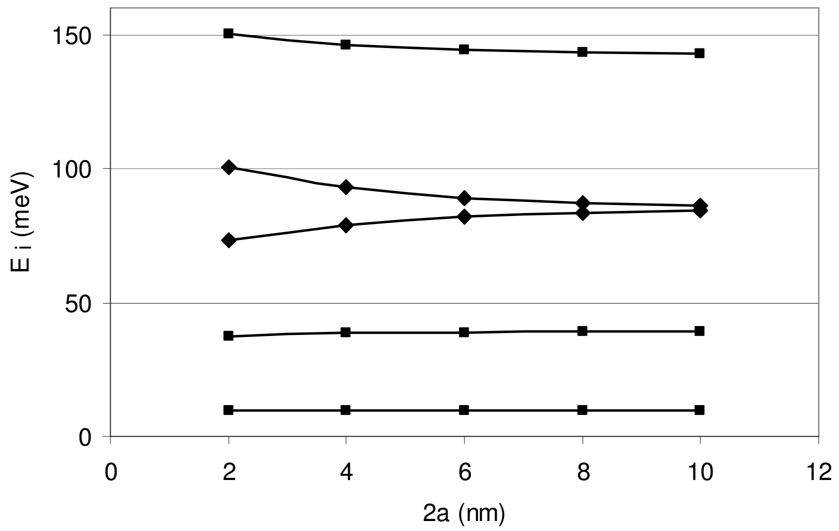

FIG 4. Energy spectra of CQW consisting of two QWs of depth 154.6 meV and widths 20 nm and 3.8 nm separated by tunnel barriers of width $2a$. See TABLE III and TABLE IV for the data.

See Figure 4, Table III and Table IV for another striking result of our extensive numerical investigations. We find that if energy of electron in two isolated QWs for motion normal to GaAs-AlGaAs interfaces happens to match for large values of barrier width $2a$ (see E_3 and E_4 in Figure 4), we find energy doublet in the energy spectra of CQW for small values of the barrier width $2a$.

IV. CONCLUSIONS

The results of numerical investigations have been found to be extremely surprising. We find that confined energy levels of individual QW become allowed energy levels in the CQW. Moreover, energy doublets form in case two isolated QWs with matching confined energy levels come close enough to create a CQW separated by a thinner tunnel barrier. We could not fathom anything like these before the numerical investigations. This paper takes readers beyond their existing knowledge on the topic. Calculations are orthodox but results are novel. The energy spectrum is readily verifiable by optical experiments. This is a fundamental and novel contribution to pure Nanostructure Physics.

V. REFERENCES

[1] D. K. Ferry, S. M. Goodnick, Transport in Nanostructures, 1st edn. (Cambridge University Press, Cambridge, 1997)
[2] S. Chowdhury, M. J. Iqbal, Nanostructure Physics of Coupled Quantum Well, 1st edn. (American Academic Press, Utah, 2015)
[3] S. Chowdhury, M. Rahman, Non-Tunneling Regime of Coupled Quantum Well 1st edn. (American Academic Press, Utah, 2016)
[4] U. K. Chowdhury, S. Chowdhury, Coupled Quantum Well in Longitudinal Magnetic Field, 1st edn. (American Academic Press, Utah, 2017)
[5] U. K. Chowdhury, S. Chowdhury, M. J. Iqbal, Physica E **117** (2020) 113796
[6] S. Chowdhury, Quantum Mechanics, 1st edn. (Narosa / Alpha Science, 2014)
[7] W. L. Bloss, Journal of Applied Physics **67** (1990) 1421
[8] B. Olejnikova, Semiconductor Science and Technology **8** (1993) 525
[9] S. S. Dash, S. Chowdhury, Nanostructure Physics of Isolated Quantum Well, 1st edn. (Lambert Academic Publishing, Germany, 2010)
[10] S. Chowdhury, Nanostructure Physics and Microelectronics, 1st edn. (Narosa / Alpha Science, 2014)
[11] S. Chowdhury, Computational Physics, 1st edn. (American Academic Press, Utah, 2021)

10.29322/IJSRP.15.11.2025.p16747

Data availability: Available in the paper and in the supplementary material.

Competing interest: None

Author contributions: All authors contributed to the study, conceptualization, data collection and analysis. The first draft of the manuscript was written by Sujaul Chowdhury. Shahriar Pollob commented on it. All authors have read and approved the final manuscript.

Supplementary Material:

Chapter I contains analytical calculations and includes Figure S1.1 to S1.3

Chapter II contains numerical investigations and includes Figure S2.1 to S2.22 and Table S2.1 to S2.36

Funding: None

Supplementary Materials for

Energy spectrum of GaAs-AlGaAs Coupled Quantum Well

Shahriar Pollob, Sujaul Chowdhury*

*Corresponding author: s.chowdhury-phy@sust.edu

*https://orcid.org/0000-0001-6862-9989

The PDF file includes:

Analytical calculation
Numerical investigation
Figs. S1.1 to S1.3 and S2.1 to S2.22
Tables S2.1 to S2.36

Chapter I

Analytical calculation of transcendental equation obeyed by quasi-bound energy levels of Coupled Quantum Well

1.1 Introduction to the problem

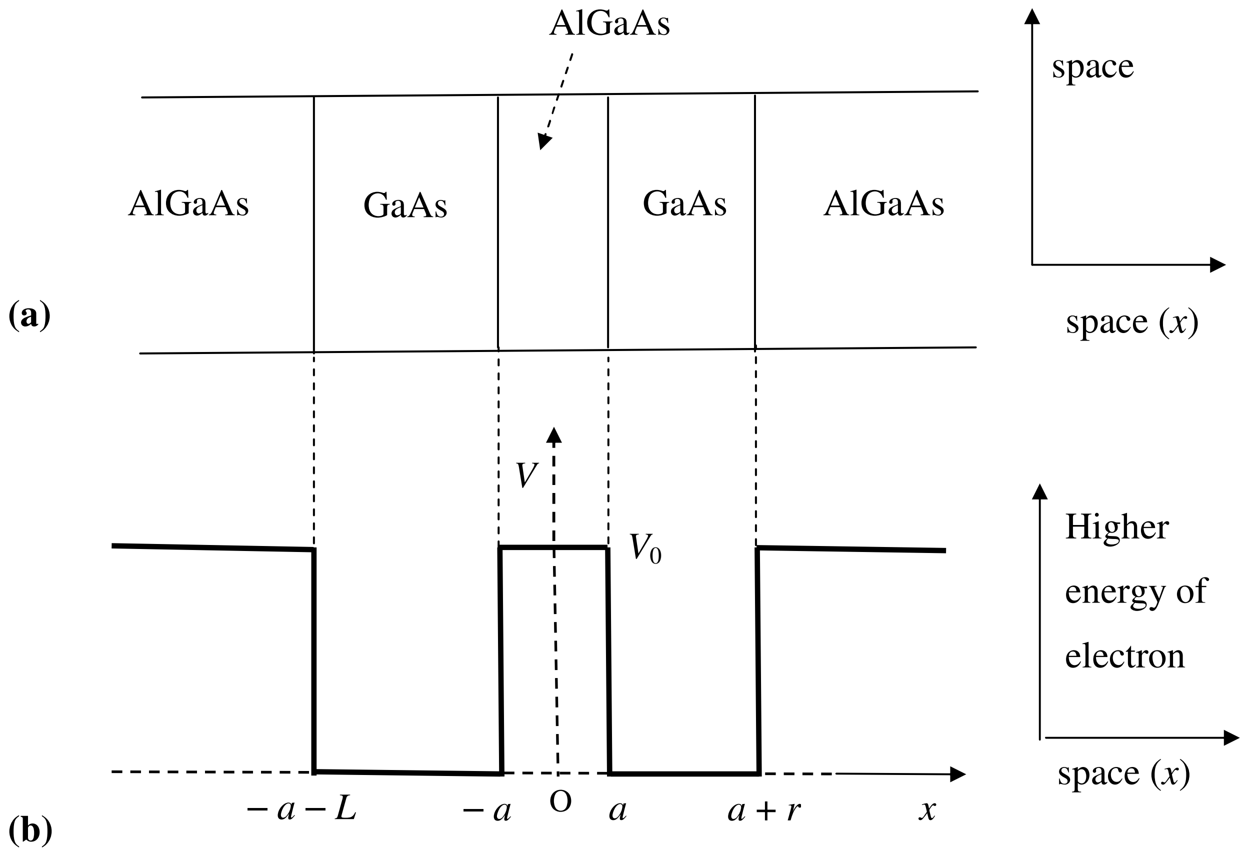

Figure S1.1 (a) Material structure (b) band model of GaAs-AlGaAs Coupled Quantum Well. O is origin (0, 0) of the coordinate system. Potential energy V is zero in the Quantum Wells because of the choice of origin. QW widths L and r are different.

As Figure S1.1 shows, we have 2 Quantum Wells of unequal widths L and r and equal depth V_0 separated by a tunnel barrier of width $2a$ and height V_0. Widths $2a$, L and r are small and nano-scale. Hence we have a nanostructure here. The Quantum Wells are not isolated Quantum Wells because an electron residing in one Quantum Well can tunnel the thin barrier and can go to the neighboring Quantum Well. On the other sides of the Quantum Wells, we have AlGaAs barrier layers of semi-infinite thickness. Matter wave associated with an electron residing in this nanostructure can feel the barrier and both the wells at a time.

In this chapter, we obtain a transcendental equation obeyed by quasi-bound energy levels of the Coupled Quantum Well. The energy levels are in fact allowed values of kinetic energy of electron in GaAs Quantum Well layers for motion perpendicular to GaAs-AlGaAs interfaces i.e. for motion along x direction. This is because potential energy is zero inside the Quantum Wells by choice of origin.

1.2 Transfer matrix of left half of the nanostructure

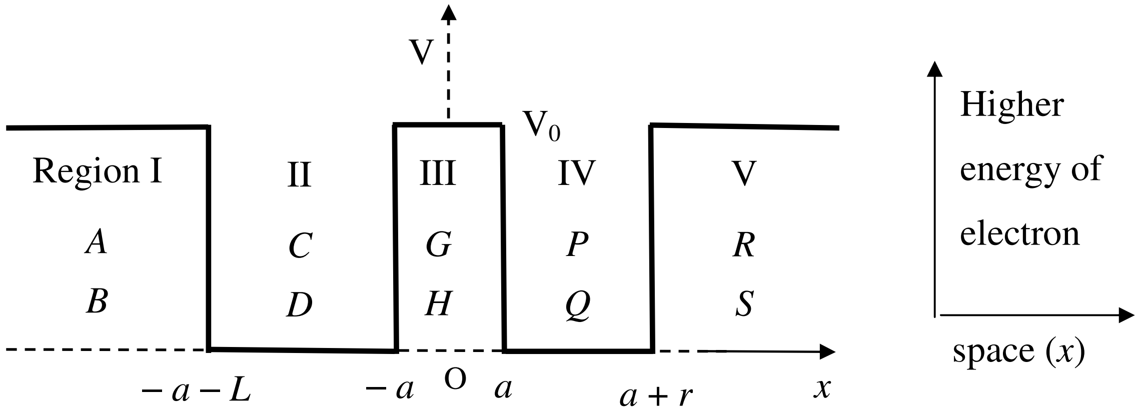

Figure S1.2 Potential energy profile for electrons in conduction band in band model of the nanostructure. Figure to help calculate transfer matrix of (left half of) the nanostructure.

Eigenvalue equation of total energy i.e. kinetic plus potential energy of an electron for motion along x direction is $[-\frac{\hbar^2}{2m}\frac{d^2}{dx^2} + V(x)]\ u(\mathrm{x}) = E\ u(x)$. u is space part of total wavefunction $\Psi(x,\ t) = u(x)e^{-\frac{i}{\hbar}Et} = u(x)\mathrm{e}^{-i\omega t}$ which is a solution of time-dependent Schroedinger equation $-\frac{\hbar^2}{2m}\frac{d^2}{dx^2}\Psi(x,\ t) + V\Psi(x,\ t) = i\hbar\frac{\partial\Psi(\mathrm{x,t})}{\partial \mathrm{t}}$.

For Quantum Well regions, we have $[-\frac{\hbar^2}{2\mathrm{m}}\frac{\mathrm{d}^2}{\mathrm{dx}^2} + 0]\ u(x) = E\ u(x)$. This is eigenvalue equation of kinetic energy operator. Hence E is eigenvalue or allowed value of kinetic energy of electron for motion along x direction in the Quantum Well regions. Let us write solutions to the eigenvalue equation of energy in the 5 regions as

$$u_I = Ae^{\beta x} + Be^{-\beta x} \qquad \text{----------(1.1)}$$

$$u_{II} = Ce^{i\alpha x} + De^{-i\alpha x} \qquad \text{----------(1.2)}$$

$$u_{III} = Ge^{\beta x} + He^{-\beta x} \quad \text{----------(1.3)}$$

$$u_{IV} = Pe^{i\alpha x} + Qe^{-i\alpha x} \quad \text{----------(1.4)}$$

$$u_{V} = Re^{\beta x} + Se^{-\beta x} \quad \text{----------(1.5)}$$

where $$\alpha^2 = \frac{2mE}{\hbar^2} \quad \text{----------(1.6)}$$

and $$\beta^2 = \frac{2m}{\hbar^2}(V_0 - E) \quad \text{----------(1.7)}$$

We have boundary condition $u_{II} = u_{III}$ at $x = -a$ which gives

$$Ce^{i\alpha x} + De^{-i\alpha x} = Ge^{\beta x} + He^{-\beta x} \quad \text{at } x = -a$$

or, $Ce^{-i\alpha a} + De^{i\alpha a} = Ge^{-\beta a} + He^{\beta a}$

or, $$Ge^{-\beta a} + He^{\beta a} = Ce^{-i\alpha a} + De^{i\alpha a} \quad \text{----------(1.8)}$$

We also have boundary condition $\frac{du_{II}}{dx} = \frac{du_{III}}{dx}$ at $x = -a$ which gives

$$i\alpha Ce^{i\alpha x} - i\alpha De^{-i\alpha x} = \beta Ge^{\beta x} - \beta He^{-\beta x} \quad \text{at } x = -a$$

or, $i\alpha Ce^{-i\alpha a} - i\alpha De^{i\alpha a} = \beta Ge^{-\beta a} - \beta He^{\beta a}$

or, $$Ge^{-\beta a} - He^{\beta a} = \frac{i\alpha}{\beta}Ce^{-i\alpha a} - \frac{i\alpha}{\beta}De^{i\alpha a} \quad \text{----------(1.9)}$$

Equation (1.8) + (1.9) gives

$$2Ge^{-\beta a} = C\left(e^{-i\alpha a} + \frac{i\alpha}{\beta}e^{-i\alpha a}\right) + D\left(e^{i\alpha a} - \frac{i\alpha}{\beta}e^{i\alpha a}\right)$$

or, $$G = C\frac{1}{2}\left(e^{-i\alpha a} + \frac{i\alpha}{\beta}e^{-i\alpha a}\right)e^{\beta a} + D\frac{1}{2}\left(e^{i\alpha a} - \frac{i\alpha}{\beta}e^{i\alpha a}\right)e^{\beta a} \quad \text{----------(1.10)}$$

Equation (1.8) – (1.9) gives

$$2He^{\beta a} = C\left(e^{-i\alpha a} - \frac{i\alpha}{\beta}e^{-i\alpha a}\right) + D\left(e^{i\alpha a} + \frac{i\alpha}{\beta}e^{i\alpha a}\right)$$

or, $$H = C\frac{1}{2}\left(e^{-i\alpha a} - \frac{i\alpha}{\beta}e^{-i\alpha a}\right)e^{-\beta a} + D\frac{1}{2}\left(e^{i\alpha a} + \frac{i\alpha}{\beta}e^{i\alpha a}\right)e^{-\beta a} \quad \text{----------(1.11)}$$

10.29322/IJSRP.15.11.2025.p16747

Equation (1.10) and (1.11) give

$$\begin{pmatrix} G \\ H \end{pmatrix} = \begin{pmatrix} \frac{1}{2}\left(e^{-i\alpha a} + \frac{i\alpha}{\beta} e^{-i\alpha a}\right)e^{\beta a} & \frac{1}{2}\left(e^{i\alpha a} - \frac{i\alpha}{\beta} e^{i\alpha a}\right)e^{\beta a} \\ \frac{1}{2}\left(e^{-i\alpha a} - \frac{i\alpha}{\beta} e^{-i\alpha a}\right)e^{-\beta a} & \frac{1}{2}\left(e^{i\alpha a} + \frac{i\alpha}{\beta} e^{i\alpha a}\right)e^{-\beta a} \end{pmatrix} \begin{pmatrix} C \\ D \end{pmatrix} \qquad \text{----------(1.12)}$$

Again, we have boundary condition $u_{\mathrm{I}} = u_{\mathrm{II}}$ at $x = -a - L$ which gives

$$Ae^{\beta x} + Be^{-\beta x} = Ce^{i\alpha x} + De^{-i\alpha x} \qquad \text{at } x = -a - L$$

or, $Ae^{-\beta(a+L)} + Be^{\beta(a+L)} = Ce^{-i\alpha(a+L)} + De^{i\alpha(a+L)}$

or, $Ce^{-i\alpha(a+L)} + De^{i\alpha(a+L)} = Ae^{-\beta(a+L)} + Be^{\beta(a+L)}$ ----------(1.13)

We also have boundary condition $\frac{du_I}{dx} = \frac{du_{II}}{dx}$ at $x = -a - L$ which gives

$$\beta Ae^{\beta x} - \beta Be^{-\beta x} = i\alpha Ce^{i\alpha x} - i\alpha De^{-i\alpha x} \qquad \text{at } x = -a - L$$

or, $\beta Ae^{-\beta(a+L)} - \beta Be^{\beta(a+L)} = i\alpha Ce^{-i\alpha(a+L)} - i\alpha De^{i\alpha(a+L)}$

or, $Ce^{-i\alpha(a+L)} - De^{i\alpha(a+L)} = \frac{\beta}{i\alpha} Ae^{-\beta(a+L)} - \frac{\beta}{i\alpha} Be^{\beta(a+L)}$ ----------(1.14)

Equation (1.13) + (1.14) gives

$$2Ce^{-i\alpha(a+L)} = A\left(e^{-\beta(a+L)} + \frac{\beta}{i\alpha} e^{-\beta(a+L)}\right) + B\left(e^{\beta(a+L)} - \frac{\beta}{i\alpha} e^{\beta(a+L)}\right)$$

or,

$$C = A\frac{1}{2}\left(e^{-\beta(a+L)} + \frac{\beta}{i\alpha} e^{-\beta(a+L)}\right)e^{i\alpha(a+L)} + B\frac{1}{2}\left(e^{\beta(a+L)} - \frac{\beta}{i\alpha} e^{\beta(a+L)}\right)e^{i\alpha(a+L)}$$

----------(1.15)

Equation (1.13) − (1.14) gives

$$2De^{i\alpha(a+L)} = A\left(e^{-\beta(a+L)} - \frac{\beta}{i\alpha} e^{-\beta(a+L)}\right) + B\left(e^{\beta(a+L)} + \frac{\beta}{i\alpha} e^{\beta(a+L)}\right)$$

or,

$$D = A\frac{1}{2}\left(e^{-\beta(a+L)} - \frac{\beta}{i\alpha} e^{-\beta(a+L)}\right)e^{-i\alpha(a+L)} + B\frac{1}{2}\left(e^{\beta(a+L)} + \frac{\beta}{i\alpha} e^{\beta(a+L)}\right)e^{-i\alpha(a+L)}$$

----------(1.16)

10.29322/IJSRP.15.11.2025.p16747

Equation (1.15) and (1.16) give

$$\begin{pmatrix} C \\ D \end{pmatrix} = \begin{pmatrix} \frac{1}{2}\left(e^{-\beta(a+L)}+\frac{\beta}{i\alpha}e^{-\beta(a+L)}\right)e^{i\alpha(a+L)} & \frac{1}{2}\left(e^{\beta(a+L)}-\frac{\beta}{i\alpha}e^{\beta(a+L)}\right)e^{i\alpha(a+L)} \\ \frac{1}{2}\left(e^{-\beta(a+L)}-\frac{\beta}{i\alpha}e^{-\beta(a+L)}\right)e^{-i\alpha(a+L)} & \frac{1}{2}\left(e^{\beta(a+L)}+\frac{\beta}{i\alpha}e^{\beta(a+L)}\right)e^{-i\alpha(a+L)} \end{pmatrix}\begin{pmatrix} A \\ B \end{pmatrix}$$

----------(1.17)

Equation (1.12) and (1.17) give

$$\begin{pmatrix} G \\ H \end{pmatrix} = \begin{pmatrix} T_{L11} & T_{L12} \\ T_{L21} & T_{L22} \end{pmatrix}\begin{pmatrix} A \\ B \end{pmatrix} \qquad \text{---------(1.18)}$$

Here the square matrix is transfer matrix of left half of the nanostructure; see Figure S1.2. Here equation (1.12), (1.17) and (1.18) give

$$T_{\mathrm{L}11} = \frac{1}{2}\left(e^{-i\alpha a}+\frac{i\alpha}{\beta}e^{-i\alpha a}\right)e^{\beta a}\,\frac{1}{2}\left(e^{-\beta(a+L)}+\frac{\beta}{i\alpha}e^{-\beta(a+L)}\right)e^{i\alpha(a+L)}$$

$$+\frac{1}{2}\left(e^{i\alpha a}-\frac{i\alpha}{\beta}e^{i\alpha a}\right)e^{\beta a}\,\frac{1}{2}\left(e^{-\beta(a+L)}-\frac{\beta}{i\alpha}e^{-\beta(a+L)}\right)e^{-i\alpha(a+L)}$$

or, $$T_{\mathrm{L}11} = \frac{1}{4}\left(1+\frac{i\alpha}{\beta}\right)e^{-i\alpha a}e^{\beta a}\left(1+\frac{\beta}{i\alpha}\right)e^{-\beta(a+L)}e^{i\alpha(a+L)}$$

$$+\frac{1}{4}\left(1-\frac{i\alpha}{\beta}\right)e^{i\alpha a}e^{\beta a}\left(1-\frac{\beta}{i\alpha}\right)e^{-\beta(a+L)}e^{-i\alpha(a+L)}$$

or, $$T_{\mathrm{L}11} = \frac{1}{4}\left(2+\frac{i\alpha}{\beta}+\frac{\beta}{i\alpha}\right)e^{i\alpha L}e^{-\beta L}+\frac{1}{4}\left(2-\frac{i\alpha}{\beta}-\frac{\beta}{i\alpha}\right)e^{-i\alpha L}e^{-\beta L}$$

or, $$T_{\mathrm{L}11} = \frac{1}{4}\left(2+i\left(\frac{\alpha}{\beta}-\frac{\beta}{\alpha}\right)\right)e^{i\alpha L}e^{-\beta L}+\frac{1}{4}\left(2-i\left(\frac{\alpha}{\beta}-\frac{\beta}{\alpha}\right)\right)e^{-i\alpha L}e^{-\beta L} \qquad \text{---------(1.19)}$$

Again, equation (1.12), (1.17) and (1.18) give

$$T_{\mathrm{L}21} = \frac{1}{2}\left(e^{-i\alpha a}-\frac{i\alpha}{\beta}e^{-i\alpha a}\right)e^{-\beta a}\,\frac{1}{2}\left(e^{-\beta(a+L)}+\frac{\beta}{i\alpha}e^{-\beta(a+L)}\right)e^{i\alpha(a+L)}$$

$$+\frac{1}{2}\left(e^{i\alpha a}+\frac{i\alpha}{\beta}e^{i\alpha a}\right)e^{-\beta a}\,\frac{1}{2}\left(e^{-\beta(a+L)}-\frac{\beta}{i\alpha}e^{-\beta(a+L)}\right)e^{-i\alpha(a+L)}$$

$$\text{or, } T_{L21} = \frac{1}{4}\left(1-\frac{i\alpha}{\beta}\right)e^{-i\alpha a}e^{-\beta a}\left(1+\frac{\beta}{i\alpha}\right)e^{-\beta(a+L)}e^{i\alpha(a+L)}$$

$$+\frac{1}{4}\left(1+\frac{i\alpha}{\beta}\right)e^{i\alpha a}e^{-\beta a}\left(1-\frac{\beta}{i\alpha}\right)e^{-\beta(a+L)}e^{-i\alpha(a+L)}$$

$$\text{or, } T_{L21} = -\frac{i}{4}\left(\frac{\alpha}{\beta}+\frac{\beta}{\alpha}\right)e^{-\beta(2a+L)}e^{i\alpha L} + \frac{i}{4}\left(\frac{\alpha}{\beta}+\frac{\beta}{\alpha}\right)e^{-\beta(2a+L)}e^{-i\alpha L} \qquad \text{---------(1.20)}$$

We will not need expressions for T_{L12} and T_{L22}.

$$T_{L12} = \ldots \qquad \text{---------(1.21)}$$

$$T_{L22} = \ldots \qquad \text{---------(1.22)}$$

1.3 Inverse transfer matrix of right half of the nanostructure

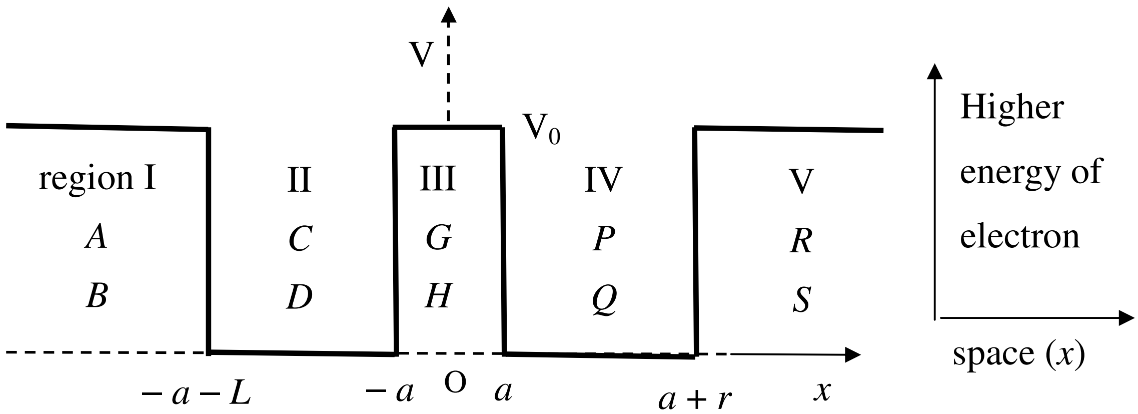

Figure S1.3 Potential energy profile for electrons in conduction band in band model of the nanostructure. Figure to help calculate inverse transfer matrix of (right half of) the nanostructure.

We have boundary condition $u_{III} = u_{IV}$ at $x = a$ which gives

$$Ge^{\beta x} + He^{-\beta x} = Pe^{i\alpha x} + Qe^{-i\alpha x} \qquad \text{at } x = a$$

$$\text{or, } Ge^{\beta a} + He^{-\beta a} = Pe^{i\alpha a} + Qe^{-i\alpha a} \qquad \text{----------(1.23)}$$

We also have boundary condition $\frac{du_{III}}{dx} = \frac{du_{IV}}{dx}$ at $x = a$ which gives

$$\beta Ge^{\beta x} - \beta He^{-\beta x} = i\alpha Pe^{i\alpha x} - i\alpha Qe^{-i\alpha x} \qquad \text{at } x = a$$

$$\text{or, } Ge^{\beta a} - He^{-\beta a} = \frac{i\alpha}{\beta}Pe^{i\alpha a} - \frac{i\alpha}{\beta}Qe^{-i\alpha a} \qquad \text{----------(1.24)}$$

Equation (1.23) +(1.24) gives

$$2Ge^{\beta a} = P\left(1+\frac{i\alpha}{\beta}\right)e^{i\alpha a} + Q\left(1-\frac{i\alpha}{\beta}\right)e^{-i\alpha a}$$

or, $$G = P\frac{1}{2}\left(1+\frac{i\alpha}{\beta}\right)e^{i\alpha a}e^{-\beta a} + Q\frac{1}{2}\left(1-\frac{i\alpha}{\beta}\right)e^{-i\alpha a}e^{-\beta a} \qquad \text{----------(1.25)}$$

Equation (1.23) − (1.24) gives

$$2He^{-\beta a} = P\left(1-\frac{i\alpha}{\beta}\right)e^{i\alpha a} + Q\left(1+\frac{i\alpha}{\beta}\right)e^{-i\alpha a}$$

or, $$H = P\frac{1}{2}\left(1-\frac{i\alpha}{\beta}\right)e^{i\alpha a}e^{\beta a} + Q\frac{1}{2}\left(1+\frac{i\alpha}{\beta}\right)e^{-i\alpha a}e^{\beta a} \qquad \text{----------(1.26)}$$

Equation (1.25) and (1.26) give

$$\begin{pmatrix} G \\ H \end{pmatrix} = \begin{pmatrix} \frac{1}{2}\left(1+\frac{i\alpha}{\beta}\right)e^{i\alpha a}e^{-\beta a} & \frac{1}{2}\left(1-\frac{i\alpha}{\beta}\right)e^{-i\alpha a}e^{-\beta a} \\ \frac{1}{2}\left(1-\frac{i\alpha}{\beta}\right)e^{i\alpha a}e^{\beta a} & \frac{1}{2}\left(1+\frac{i\alpha}{\beta}\right)e^{-i\alpha a}e^{\beta a} \end{pmatrix} \begin{pmatrix} P \\ Q \end{pmatrix} \qquad \text{----------(1.27)}$$

Again, we have boundary condition $u_{IV} = u_V$ at $x = a + r$ which gives

$$Pe^{i\alpha x} + Qe^{-i\alpha x} = Re^{\beta x} + Se^{-\beta x} \qquad \text{at } x = a + r$$

or, $$Pe^{i\alpha(a+r)} + Qe^{-i\alpha(a+r)} = Re^{\beta(a+r)} + Se^{-\beta(a+r)} \qquad \text{----------(1.28)}$$

We also have boundary condition $\frac{du_{IV}}{dx} = \frac{du_V}{dx}$ at $x = a + r$ which gives

$$i\alpha Pe^{i\alpha x} - i\alpha Qe^{-i\alpha x} = \beta Re^{\beta x} - \beta Se^{-\beta x} \qquad \text{at } x = a + r$$

or, $$i\alpha Pe^{i\alpha(a+r)} - i\alpha Qe^{-i\alpha(a+r)} = \beta Re^{\beta(a+r)} - \beta Se^{-\beta(a+r)}$$

or, $$Pe^{i\alpha(a+r)} - Qe^{-i\alpha(a+r)} = \frac{\beta}{i\alpha}Re^{\beta(a+r)} - \frac{\beta}{i\alpha}Se^{-\beta(a+r)} \qquad \text{----------(1.29)}$$

Equation (1.28) + (1.29) gives

$$2Pe^{i\alpha(a+r)} = R\left(1+\frac{\beta}{i\alpha}\right)e^{\beta(a+r)} + S\left(1-\frac{\beta}{i\alpha}\right)e^{-\beta(a+r)}$$

or, $$P = R\frac{1}{2}\left(1+\frac{\beta}{i\alpha}\right)e^{\beta(a+r)}e^{-i\alpha(a+r)} + S\frac{1}{2}\left(1-\frac{\beta}{i\alpha}\right)e^{-\beta(a+r)}e^{-i\alpha(a+r)} \qquad \text{--------(1.30)}$$

10.29322/IJSRP.15.11.2025.p16747

Equation (1.28) – (1.29) gives

$$2Qe^{-i\alpha(a+r)} = R\left(1-\frac{\beta}{i\alpha}\right)e^{\beta(a+r)} + S\left(1+\frac{\beta}{i\alpha}\right)e^{-\beta(a+r)}$$

or, $$Q = R\frac{1}{2}\left(1-\frac{\beta}{i\alpha}\right)e^{\beta(a+r)}e^{i\alpha(a+r)} + S\frac{1}{2}\left(1+\frac{\beta}{i\alpha}\right)e^{-\beta(a+r)}e^{i\alpha(a+r)} \quad \text{----------(1.31)}$$

Equation (1.30) and (1.31) give

$$\begin{pmatrix} P \\ Q \end{pmatrix} = \begin{pmatrix} \frac{1}{2}\left(1+\frac{\beta}{i\alpha}\right)e^{\beta(a+r)}e^{-i\alpha(a+r)} & \frac{1}{2}\left(1-\frac{\beta}{i\alpha}\right)e^{-\beta(a+r)}e^{-i\alpha(a+r)} \\ \frac{1}{2}\left(1-\frac{\beta}{i\alpha}\right)e^{\beta(a+r)}e^{i\alpha(a+r)} & \frac{1}{2}\left(1+\frac{\beta}{i\alpha}\right)e^{-\beta(a+r)}e^{i\alpha(a+r)} \end{pmatrix} \begin{pmatrix} R \\ S \end{pmatrix} \text{-------(1.32)}$$

Equation (1.27) and (1.32) give

$$\begin{pmatrix} G \\ H \end{pmatrix} = \begin{pmatrix} IT_{R11} & IT_{R12} \\ IT_{R21} & IT_{R22} \end{pmatrix} \begin{pmatrix} R \\ S \end{pmatrix} \quad \text{---------(1.33)}$$

Here the square matrix is inverse transfer matrix of right half of the nanostructure; see Figure S1.3. Here equation (1.27), (1.32) and (1.33) give

$$IT_{\mathrm{R22}} = \frac{1}{2}\left(1-\frac{i\alpha}{\beta}\right)e^{i\alpha a}e^{\beta a}\,\frac{1}{2}\left(1-\frac{\beta}{i\alpha}\right)e^{-\beta(a+r)}e^{-i\alpha(a+r)}$$

$$+\frac{1}{2}\left(1+\frac{i\alpha}{\beta}\right)e^{-i\alpha a}e^{\beta a}\,\frac{1}{2}\left(1+\frac{\beta}{i\alpha}\right)e^{-\beta(a+r)}e^{i\alpha(a+r)}$$

or, $$IT_{\mathrm{R22}} = \frac{1}{4}\left(2-\frac{i\alpha}{\beta}-\frac{\beta}{i\alpha}\right)e^{-\beta r}e^{-i\alpha r} + \frac{1}{4}\left(2+\frac{i\alpha}{\beta}+\frac{\beta}{i\alpha}\right)e^{-\beta r}e^{i\alpha r}$$

or, $$IT_{\mathrm{R22}} = \frac{1}{4}\left(2-i\left(\frac{\alpha}{\beta}-\frac{\beta}{\alpha}\right)\right)e^{-\beta r}e^{-i\alpha r} + \frac{1}{4}\left(2+i\left(\frac{\alpha}{\beta}-\frac{\beta}{\alpha}\right)\right)e^{-\beta r}e^{i\alpha r} \quad \text{---------(1.34)}$$

Again, equation (1.27), (1.32) and (1.33) give

$$IT_{\mathrm{R12}} = \frac{1}{2}\left(1+\frac{i\alpha}{\beta}\right)e^{i\alpha a}e^{-\beta a}\,\frac{1}{2}\left(1-\frac{\beta}{i\alpha}\right)e^{-\beta(a+r)}e^{-i\alpha(a+r)}$$

$$+\frac{1}{2}\left(1-\frac{i\alpha}{\beta}\right)e^{-i\alpha a}e^{-\beta a}\,\frac{1}{2}\left(1+\frac{\beta}{i\alpha}\right)e^{-\beta(a+r)}e^{i\alpha(a+r)}$$

or, $$IT_{\mathrm{R12}} = \frac{i}{4}\left(\frac{\alpha}{\beta}+\frac{\beta}{\alpha}\right)e^{-\beta(2a+r)}e^{-i\alpha r} - \frac{i}{4}\left(\frac{\alpha}{\beta}+\frac{\beta}{\alpha}\right)e^{-\beta(2a+r)}e^{i\alpha r} \quad \text{---------(1.35)}$$

We will not need expressions for IT_{R11} and IT_{R21}.

$IT_{R11} = \ldots$ ---------(1.36)

$IT_{R21} = \ldots$ ---------(1.37)

1.4 Calculation of transcendental equation obeyed by quasi-bound energy levels of Coupled Quantum Well

Equation (1.18) and (1.33) give

$$\begin{pmatrix} T_{L11} & T_{L12} \\ T_{L21} & T_{L22} \end{pmatrix} \begin{pmatrix} A \\ B \end{pmatrix} = \begin{pmatrix} IT_{R11} & IT_{R12} \\ IT_{R21} & IT_{R22} \end{pmatrix} \begin{pmatrix} R \\ S \end{pmatrix} \qquad \text{---------(1.38)}$$

In view of $u_I = Ae^{\beta x} + Be^{-\beta x}$ and band model of Figure S1.2, we stipulate that $B = 0$; otherwise the term $Be^{-\beta x} \to \infty$ as $x \to -\infty$ which violates admissibility condition of wavefunction. Again, in view of $u_V = Re^{\beta x} + Se^{-\beta x}$ and band model of Figure S1.2, we stipulate that $R = 0$; otherwise the term $Re^{\beta x} \to \infty$ as $x \to +\infty$ which violates admissibility condition of wavefunction.

Use of $B = 0$ and $R = 0$ in equation (1.38) gives

$$\begin{pmatrix} T_{L11} & T_{L12} \\ T_{L21} & T_{L22} \end{pmatrix} \begin{pmatrix} A \\ 0 \end{pmatrix} = \begin{pmatrix} IT_{R11} & IT_{R12} \\ IT_{R21} & IT_{R22} \end{pmatrix} \begin{pmatrix} 0 \\ S \end{pmatrix}$$

or, $T_{L11} A + 0 = 0 + IT_{R12} S$ ---------(1.39)

and $T_{L21} A + 0 = 0 + IT_{R22} S$ ---------(1.40)

Dividing equation (1.39) by (1.40), we get

$$\frac{T_{L11}}{T_{L21}} = \frac{IT_{R12}}{IT_{R22}}$$

or, $T_{L11} IT_{R22} = T_{L21} IT_{R12}$ ---------(1.41)

Equation (1.41), (1.19), (1.34), (1.20), (1.35) give

$$\left[\frac{1}{4}\left(2 + i\left(\frac{\alpha}{\beta} - \frac{\beta}{\alpha}\right)\right)e^{i\alpha L}e^{-\beta L} + \frac{1}{4}\left(2 - i\left(\frac{\alpha}{\beta} - \frac{\beta}{\alpha}\right)\right)e^{-i\alpha L}e^{-\beta L}\right]$$

$$\left[\frac{1}{4}\left(2 - i\left(\frac{\alpha}{\beta} - \frac{\beta}{\alpha}\right)\right)e^{-\beta r}e^{-i\alpha r} + \frac{1}{4}\left(2 + i\left(\frac{\alpha}{\beta} - \frac{\beta}{\alpha}\right)\right)e^{-\beta r}e^{i\alpha r}\right]$$

10.29322/IJSRP.15.11.2025.p16747

$$=\left[-\frac{i}{4}\left(\frac{\alpha}{\beta}+\frac{\beta}{\alpha}\right)e^{-\beta(2a+L)}e^{i\alpha L}\quad+\frac{i}{4}\left(\frac{\alpha}{\beta}+\frac{\beta}{\alpha}\right)e^{-\beta(2a+L)}e^{-i\alpha L}\right]$$

$$\left[\frac{i}{4}\left(\frac{\alpha}{\beta}+\frac{\beta}{\alpha}\right)e^{-\beta(2a+r)}e^{-i\alpha r}\quad-\frac{i}{4}\left(\frac{\alpha}{\beta}+\frac{\beta}{\alpha}\right)e^{-\beta(2a+r)}e^{i\alpha r}\right]$$

or,

$$\begin{aligned}
&\frac{1}{16}\left\{4+\left(\frac{\alpha}{\beta}-\frac{\beta}{\alpha}\right)^2\right\}e^{i\alpha(L-r)}e^{-\beta(L+r)}\\
&+\frac{1}{16}\left\{4+\left(\frac{\alpha}{\beta}-\frac{\beta}{\alpha}\right)^2\right\}e^{-i\alpha(L-r)}e^{-\beta(L+r)}\\
&+\frac{1}{16}\left\{4-\left(\frac{\alpha}{\beta}-\frac{\beta}{\alpha}\right)^2+i4\left(\frac{\alpha}{\beta}-\frac{\beta}{\alpha}\right)\right\}e^{i\alpha(L+r)}e^{-\beta(L+r)}\\
&+\frac{1}{16}\left\{4-\left(\frac{\alpha}{\beta}-\frac{\beta}{\alpha}\right)^2-i4\left(\frac{\alpha}{\beta}-\frac{\beta}{\alpha}\right)\right\}e^{-i\alpha(L+r)}e^{-\beta(L+r)}\\
=&\frac{1}{16}\left(\frac{\alpha}{\beta}+\frac{\beta}{\alpha}\right)^2e^{i\alpha(L-r)}e^{-\beta(4a+L+r)}\\
&+\frac{1}{16}\left(\frac{\alpha}{\beta}+\frac{\beta}{\alpha}\right)^2e^{-i\alpha(L-r)}e^{-\beta(4a+L+r)}\\
&-\frac{1}{16}\left(\frac{\alpha}{\beta}+\frac{\beta}{\alpha}\right)^2e^{i\alpha(L+r)}e^{-\beta(4a+L+r)}\\
&-\frac{1}{16}\left(\frac{\alpha}{\beta}+\frac{\beta}{\alpha}\right)^2e^{-i\alpha(L+r)}e^{-\beta(4a+L+r)}
\end{aligned}\qquad\text{---------(1.42)}$$

10.29322/IJSRP.15.11.2025.p16747

We now equate imaginary parts of equation (1.42), and get

$$\left\{4+\left(\frac{\alpha}{\beta}-\frac{\beta}{\alpha}\right)^2\right\}e^{-\beta(L+r)}\sin\left(\alpha(L-r)\right)$$
$$-\left\{4+\left(\frac{\alpha}{\beta}-\frac{\beta}{\alpha}\right)^2\right\}e^{-\beta(L+r)}\sin\left(\alpha(L-r)\right)$$
$$+\left\{4-\left(\frac{\alpha}{\beta}-\frac{\beta}{\alpha}\right)^2\right\}e^{-\beta(L+r)}\sin\left(\alpha(L+r)\right)$$
$$+4\left(\frac{\alpha}{\beta}-\frac{\beta}{\alpha}\right)e^{-\beta(L+r)}\cos\left(\alpha(L+r)\right)$$
$$-\left\{4-\left(\frac{\alpha}{\beta}-\frac{\beta}{\alpha}\right)^2\right\}e^{-\beta(L+r)}\sin\left(\alpha(L+r)\right)$$
$$-4\left(\frac{\alpha}{\beta}-\frac{\beta}{\alpha}\right)e^{-\beta(L+r)}\cos\left(\alpha(L+r)\right)$$
$$=\left(\frac{\alpha}{\beta}+\frac{\beta}{\alpha}\right)^2 e^{-\beta(4a+L+r)}\sin\left(\alpha(L-r)\right)$$
$$-\left(\frac{\alpha}{\beta}+\frac{\beta}{\alpha}\right)^2 e^{-\beta(4a+L+r)}\sin\left(\alpha(L-r)\right)$$
$$-\left(\frac{\alpha}{\beta}+\frac{\beta}{\alpha}\right)^2 e^{-\beta(4a+L+r)}\sin\left(\alpha(L+r)\right)$$
$$+\left(\frac{\alpha}{\beta}+\frac{\beta}{\alpha}\right)^2 e^{-\beta(4a+L+r)}\sin\left(\alpha(L+r)\right)$$

or, $0 = 0$

This is a trivial result.

10.29322/IJSRP.15.11.2025.p16747

We now equate real parts of equation (1.42), and get

$$\left\{4+\left(\frac{\alpha}{\beta}-\frac{\beta}{\alpha}\right)^2\right\}e^{-\beta(L+r)}\cos\left(\alpha(L-r)\right.$$
$$+\left\{4+\left(\frac{\alpha}{\beta}-\frac{\beta}{\alpha}\right)^2\right\}e^{-\beta(L+r)}\cos\left(\alpha(L-r)\right)$$
$$+\left\{4-\left(\frac{\alpha}{\beta}-\frac{\beta}{\alpha}\right)^2\right\}e^{-\beta(L+r)}\cos\left(\alpha(L+r)\right)$$
$$-4\left(\frac{\alpha}{\beta}-\frac{\beta}{\alpha}\right)e^{-\beta(L+r)}\sin\left(\alpha(L+r)\right)$$
$$+\left\{4-\left(\frac{\alpha}{\beta}-\frac{\beta}{\alpha}\right)^2\right\}e^{-\beta(L+r)}\cos\left(\alpha(L+r)\right)$$
$$-4\left(\frac{\alpha}{\beta}-\frac{\beta}{\alpha}\right)e^{-\beta(L+r)}\sin\left(\alpha(L+r)\right)$$
$$=\left(\frac{\alpha}{\beta}+\frac{\beta}{\alpha}\right)^2 e^{-\beta(4a+L+r)}\cos\left(\alpha(L-r)\right)$$
$$+\left(\frac{\alpha}{\beta}+\frac{\beta}{\alpha}\right)^2 e^{-\beta(4a+L+r)}\cos\left(\alpha(L-r)\right)$$
$$-\left(\frac{\alpha}{\beta}+\frac{\beta}{\alpha}\right)^2 e^{-\beta(4a+L+r)}\cos\left(\alpha(L+r)\right)$$
$$-\left(\frac{\alpha}{\beta}+\frac{\beta}{\alpha}\right)^2 e^{-\beta(4a+L+r)}\cos\left(\alpha(L+r)\right)$$

or,

$$2\left\{4+\left(\frac{\alpha}{\beta}-\frac{\beta}{\alpha}\right)^2\right\}e^{-\beta(L+r)}\cos\left(\alpha(L-r)\right)$$
$$+2\left\{4-\left(\frac{\alpha}{\beta}-\frac{\beta}{\alpha}\right)^2\right\}e^{-\beta(L+r)}\cos\left(\alpha(L+r)\right)$$
$$-8\left(\frac{\alpha}{\beta}-\frac{\beta}{\alpha}\right)e^{-\beta(L+r)}\sin\left(\alpha(L+r)\right)$$
$$-2\left(\frac{\alpha}{\beta}+\frac{\beta}{\alpha}\right)^2 e^{-\beta(4a+L+r)}\cos\left(\alpha(L-r)\right)$$
$$+2\left(\frac{\alpha}{\beta}+\frac{\beta}{\alpha}\right)^2 e^{-\beta(4a+L+r)}\cos\left(\alpha(L+r)\right)$$
$$=0$$

10.29322/IJSRP.15.11.2025.p16747

or,

$$\left\{4+\left(\frac{\alpha}{\beta}-\frac{\beta}{\alpha}\right)^2\right\}\cos\left(\alpha(L-r)\right)$$
$$+\left\{4-\left(\frac{\alpha}{\beta}-\frac{\beta}{\alpha}\right)^2\right\}\cos\left(\alpha(L+r)\right)$$
$$-4\left(\frac{\alpha}{\beta}-\frac{\beta}{\alpha}\right)\sin\left(\alpha(L+r)\right)$$
$$-\left(\frac{\alpha}{\beta}+\frac{\beta}{\alpha}\right)^2 e^{-\beta(4a)}\cos\left(\alpha(L-r)\right)$$
$$+\left(\frac{\alpha}{\beta}+\frac{\beta}{\alpha}\right)^2 e^{-\beta(4a)}\cos\left(\alpha(L+r)\right)$$
$$=0$$

---------**(1.43)**

This is the transcendental equation obeyed by quasi-bound energy levels of an electron residing in Coupled Quantum Well.

10.29322/IJSRP.15.11.2025.p16747

Chapter II

Numerical investigation of parametric variations of quasi-bound energy levels of Coupled Quantum Well

10.29322/IJSRP.15.11.2025.p16747

Energy spectrum of GaAs-AlGaAs Coupled Quantum Well

2.1 The transcendental equation obeyed by quasi-bound energy levels of coupled Quantum Well

The equation is Equation (1.43):

$$\begin{aligned} \mathrm{G} = &\left\{4+\left(\frac{\alpha}{\beta}-\frac{\beta}{\alpha}\right)^2\right\}\cos\left(\alpha(L-r)\right) \\ &+\left\{4-\left(\frac{\alpha}{\beta}-\frac{\beta}{\alpha}\right)^2\right\}\cos\left(\alpha(L+r)\right) \\ &-4\left(\frac{\alpha}{\beta}-\frac{\beta}{\alpha}\right)\sin\left(\alpha(L+r)\right) \\ &-\left(\frac{\alpha}{\beta}+\frac{\beta}{\alpha}\right)^2 e^{-\beta(4a)}\cos\left(\alpha(L-r)\right) \\ &+\left(\frac{\alpha}{\beta}+\frac{\beta}{\alpha}\right)^2 e^{-\beta(4a)}\cos\left(\alpha(L+r)\right) \\ &= 0 \end{aligned} \qquad \text{---------(2.1)}$$

where $\alpha^2 = \frac{2mE}{\hbar^2}$ and $\beta^2 = \frac{2\mathrm{m}}{\hbar^2}(\mathrm{V}_0 - \mathrm{E})$. Here $2a$ is width of the tunnel barrier separating the two Quantum Wells. L and r are widths of left and right hand Quantum Well respectively. V_0 is depth of the Quantum Wells as well as height of the tunnel barrier given by 773x meV where x is Al content of $Al_xGa_{1-x}As$. $m = 0.067m_e = 0.067\times9.1\times10^{-31}$ kg is effective mass of electron in conduction band of GaAs. See Figure S1.1.

2.2 Program and data collection

We have written program number 2.1 and plotted left hand side of equation (2.1) as a function of E for various sets of values of parameters; intersections of the curve with E axis give roots of equation (2.1) which we found out by the so called bisection method.

As to isolated Quantum Wells of width b and depth V_0, we have obtained energy spectrum by graphical solutions of the two transcendental equations

$$\tan\left(\frac{\mathrm{b}}{2}\sqrt{\frac{2\mathrm{mE}}{\hbar^2}}\right) = \sqrt{\frac{\mathrm{V}_0}{\mathrm{E}}-1} \quad \text{and} \quad -\cot\left(\frac{\mathrm{b}}{2}\sqrt{\frac{2\mathrm{mE}}{\hbar^2}}\right) = \sqrt{\frac{\mathrm{V}_0}{\mathrm{E}}-1}$$

following S. S. Dash and S. Chowdhury, Lambert Academic Publishing (2010).

10.29322/IJSRP.15.11.2025.p16747

program number 2.1

part A

```
a=1*10^-9
L=20*10^-9
r=15*10^-9
x=0.4

m=0.067*9.1*10^-31
V0=773*x
hcut=(6.626*10^-34)/(2*3.1416)
alpha=Sqrt[2*m*X*1.6*10^-22/hcut^2]
beta=Sqrt[2*m*(V0-X)*1.6*10^-22/hcut^2]

G=(4+(alpha/beta-beta/alpha)^2)*Cos[alpha*(L-r)]+
(4-(alpha/beta-beta/alpha)^2)*Cos[alpha*(L+r)]-
4*(alpha/beta-beta/alpha)*Sin[alpha*(L+r)]-
((alpha/beta+beta/alpha)^2)*Exp[-4*a*beta]*Cos[alpha*(L-r)]+
((alpha/beta+beta/alpha)^2)*Exp[-4*a*beta]*Cos[alpha*(L+r)]

Plot[G,{X,0,V0},PlotRange->Automatic,Frame->True,
FrameTicks->All,PlotStyle->{Black},FrameLabel->{"E (meV)","G "}]
```

part B

```
X[1]=60
X[2]=70

i=0
```


10.29322/IJSRP.15.11.2025.p16747

```
Do[
alpha1=Sqrt[2*m*X[1]*1.6*10^-22/hcut^2];
alpha2=Sqrt[2*m*X[2]*1.6*10^-22/hcut^2];
beta1=Sqrt[2*m*(V0-X[1])*1.6*10^-22/hcut^2];
beta2=Sqrt[2*m*(V0-X[2])*1.6*10^-22/hcut^2];

F[1]=(4+(alpha1/beta1-beta1/alpha1)^2)*Cos[alpha1*(L-r)]+
(4-(alpha1/beta1-beta1/alpha1)^2)*Cos[alpha1*(L+r)]-
4*(alpha1/beta1-beta1/alpha1)*Sin[alpha1*(L+r)]-
((alpha1/beta1+beta1/alpha1)^2)*Exp[-4*a*beta1]*Cos[alpha1*(L-r)]+
((alpha1/beta1+beta1/alpha1)^2)*Exp[-4*a*beta1]*Cos[alpha1*(L+r)];

F[2]=(4+(alpha2/beta2-beta2/alpha2)^2)*Cos[alpha2*(L-r)]+
(4-(alpha2/beta2-beta2/alpha2)^2)*Cos[alpha2*(L+r)]-
4*(alpha2/beta2-beta2/alpha2)*Sin[alpha2*(L+r)]-
((alpha2/beta2+beta2/alpha2)^2)*Exp[-4*a*beta2]*Cos[alpha2*(L-r)]+
((alpha2/beta2+beta2/alpha2)^2)*Exp[-4*a*beta2]*Cos[alpha2*(L+r)];

i=i+1;

XBisec[i]=Xb=N[(X[1]+X[2])/2];
alphaXb=Sqrt[2*m*Xb*1.6*10^-22/hcut^2];
betaXb=Sqrt[2*m*(V0-Xb)*1.6*10^-22/hcut^2];

FBisec[i]=Fb=N[
(4+(alphaXb/betaXb-betaXb/alphaXb)^2)*Cos[alphaXb*(L-r)]+
(4-(alphaXb/betaXb-betaXb/alphaXb)^2)*Cos[alphaXb*(L+r)]-
4*(alphaXb/betaXb-betaXb/alphaXb)*Sin[alphaXb*(L+r)]-
((alphaXb/betaXb+betaXb/alphaXb)^2)*Exp[-4*a*betaXb]*
Cos[alphaXb*(L-r)]+
```

```
((alphaXb/betaXb+betaXb/alphaXb)^2)*
Exp[-4*a*betaXb]*Cos[alphaXb*(L+r)]];

p=F[1]*Fb;
If[p<0,X[2]=Xb,X[1]=Xb],{k,1,25}]

j=0;
Table[{j=j+1,XBisec[j],FBisec[j]},{j,0,24,1}];
TableForm[%,TableSpacing->{3,3},
TableHeadings->{None,{"i","E","G"}}]
```

2.3 Parametric variations of energy spectrum

Table S2.1 well widths L = 20 nm, r = 15 nm, Al content of AlGaAs x = 0.4

2a (nm)	E1 (meV)	E2 (meV)	E3 (meV)	E4 (meV)	E5 (meV)	E6 (meV)	E7 (meV)	E8 (meV)	E9 (meV)
2	10.685	17.719	42.818	69.828	96.884	151.400	175.283	250.100	281.279
4	10.876	17.862	43.317	70.698	96.720	155.139	170.391	253.475	270.871
6	10.886	17.871	43.349	70.766	96.705	155.821	169.469	255.298	266.583
8	10.887	17.871	43.351	70.771	96.703	155.914	169.334	256.103	264.924
10	10.887	17.871	43.351	70.7718	96.703	155.926	169.316	256.397	264.333

Table S2.2 isolated single QW

x = 0.4					
QW width b (nm)	E1 (meV)	E2 (meV)	E3 (meV)	E4 (meV)	E5 (meV)
15	18	71	156	264	
20	11	43	97	169	257

10.29322/IJSRP.15.11.2025.p16747

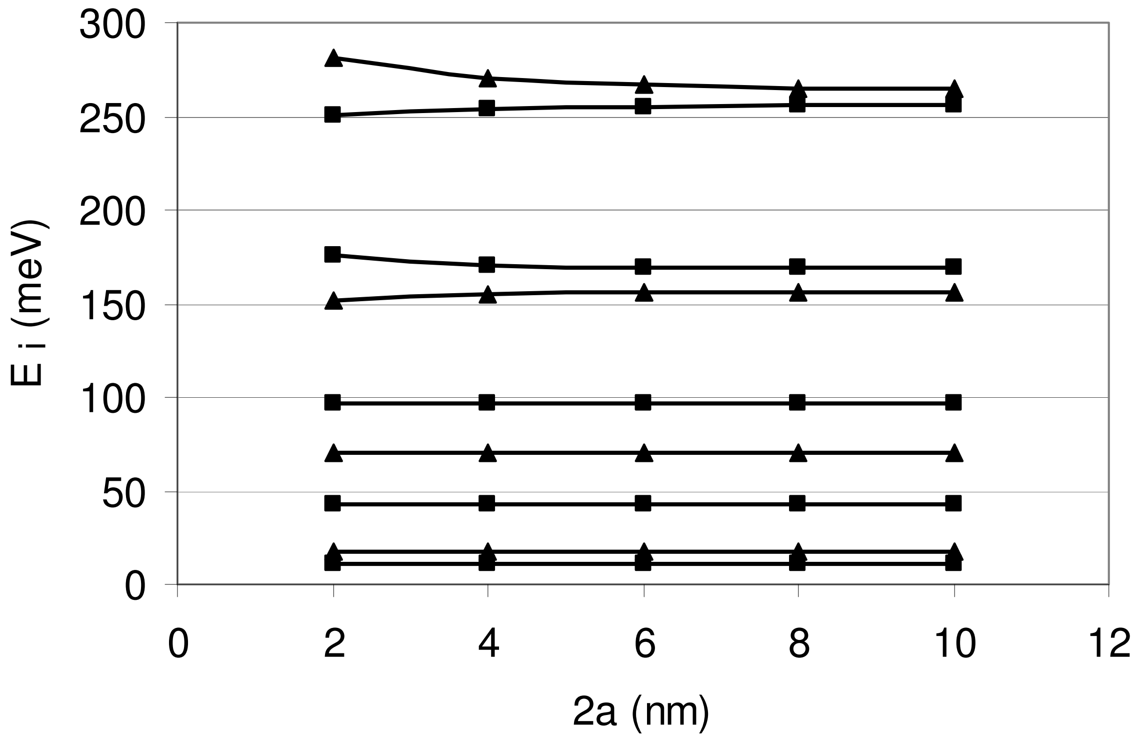

Figure S2.1 Showing data of Table S2.1: quasi-bound energy levels of Coupled Quantum Well for various widths 2a of tunnel barrier between the two wells of widths L = 20 nm and r = 15 nm and depth 773x = 309.2 meV for Al content x = 0.4 of $Al_xGa_{1-x}As$. Squares originate from isolated left hand QW and triangles originate from isolated right hand QW.

10.29322/IJSRP.15.11.2025.p16747

Table S2.3 well widths L = 20 nm, r = 10 nm, Al content of AlGaAs x = 0.4

2a (nm)	E1 (meV)	E2 (meV)	E3 (meV)	E4 (meV)	E5 (meV)	E6 (meV)	E7 (meV)	E8 (meV)
2	10.741	33.258	43.896	95.139	132.890	172.592	252.442	292.361
4	10.879	34.423	43.391	96.562	133.771	169.798	254.962	282.176
6	10.887	34.500	43.354	96.691	133.883	169.380	256.007	278.093
8	10.887	34.505	43.351	96.702	133.895	169.322	256.369	276.568
10	10.887	34.505	43.351	96.703	133.896	169.314	256.483	276.004

Table S2.4 isolated single QW

x = 0.4					
QW width b (nm)	E1 (meV)	E2 (meV)	E3 (meV)	E4 (meV)	E5 (meV)
10	35	134	276		
20	11	43	97	169	257

10.29322/IJSRP.15.11.2025.p16747

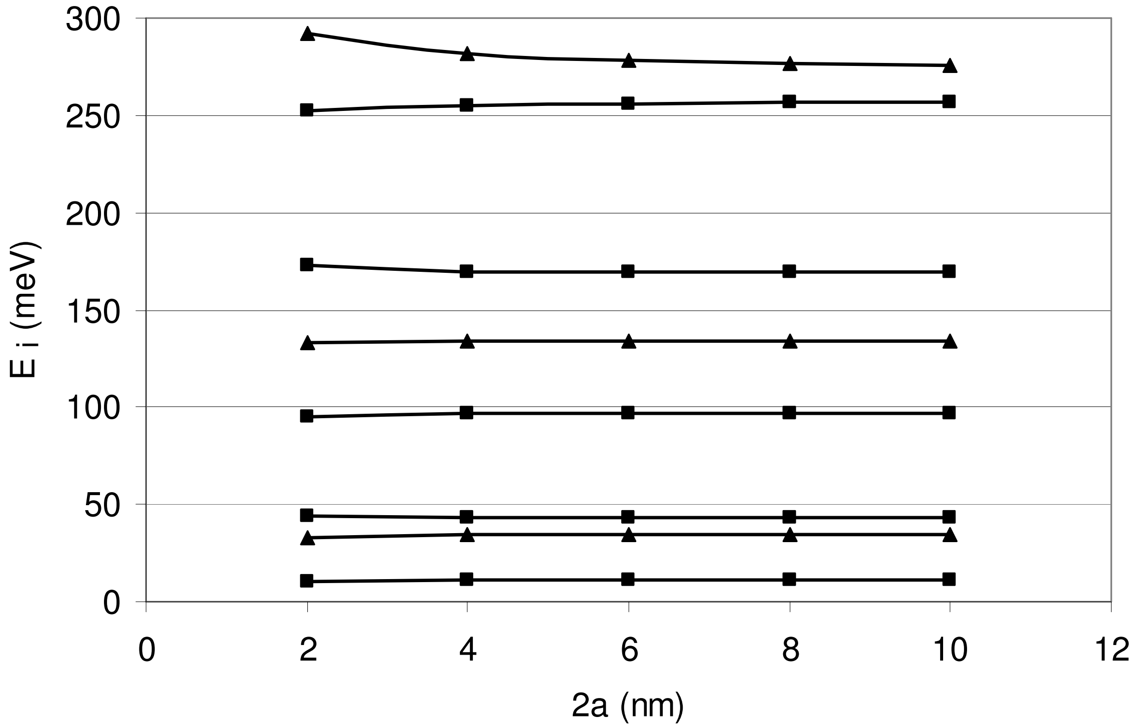

Figure S2.2 Showing data of Table S2.3: quasi-bound energy levels of Coupled Quantum Well for various widths $2a$ of tunnel barrier between the two wells of widths $L = 20$ nm and $r = 10$ nm and depth $773x = 309.2$ meV for Al content $x = 0.4$ of $Al_xGa_{1-x}As$. Squares originate from isolated left hand QW and triangles originate from isolated right hand QW.

Table S2.5 well widths L = 20 nm, r = 5 nm, Al content of AlGaAs x = 0.4

2a (nm)	E1 (meV)	E2 (meV)	E3 (meV)	E4 (meV)	E5 (meV)	E6 (meV)	E7 (meV)
2	10.781	42.607	84.057	102.804	170.798	254.606	307.789
4	10.881	43.304	89.801	97.715	169.521	255.898	301.219
6	10.887	43.348	90.732	96.805	169.341	256.336	297.417
8	10.887	43.351	90.824	96.712	169.316	256.473	295.604
10	10.887	43.351	90.831	96.704	169.313	256.514	294.741

Table S2.6 isolated single QW

x = 0.4					
QW width b (nm)	E1 (meV)	E2 (meV)	E3 (meV)	E4 (meV)	E5 (meV)
5	91	294			
20	11	43	97	169	257

10.29322/IJSRP.15.11.2025.p16747

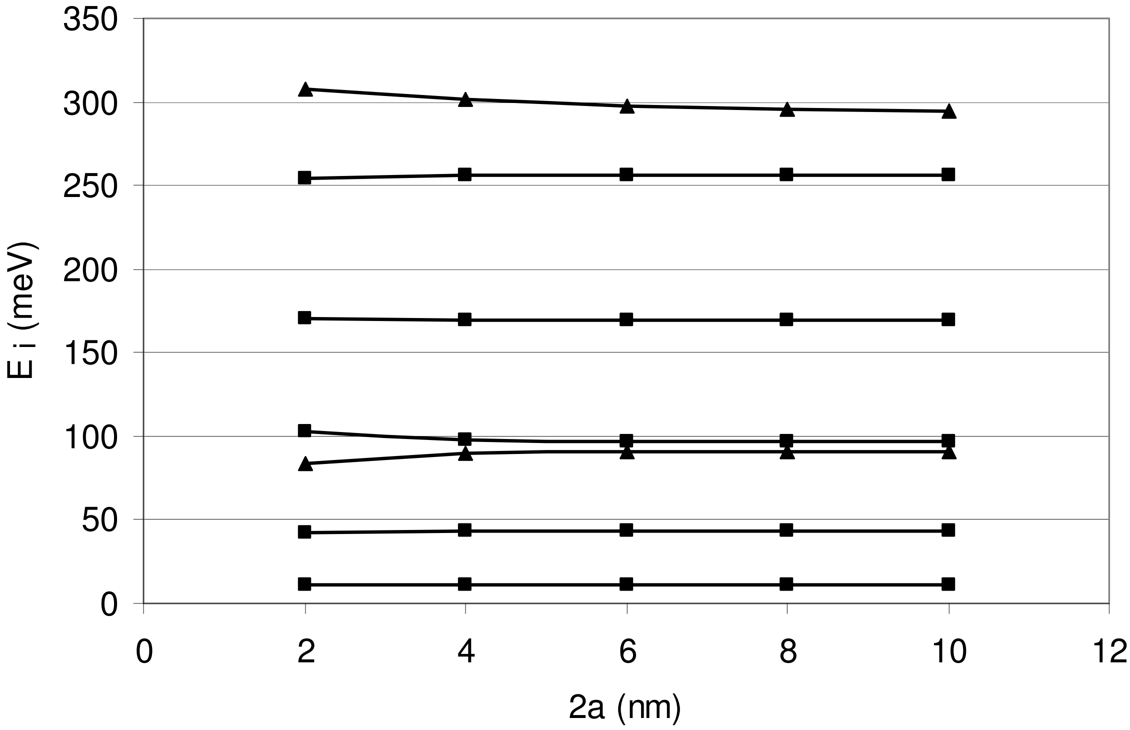

Figure S2.3 Showing data of Table S2.5: quasi-bound energy levels of Coupled Quantum Well for various widths $2a$ of tunnel barrier between the two wells of widths L = 20 nm and r = 5 nm and depth $773x$ = 309.2 meV for Al content x = 0.4 of $Al_xGa_{1-x}As$. Squares originate from isolated left hand QW and triangles originate from isolated right hand QW.

10.29322/IJSRP.15.11.2025.p16747

Table S2.7 well widths L = 20 nm, r = 15 nm, Al content of AlGaAs x = 0.3

2a (nm)	E1 (meV)	E2 (meV)	E3 (meV)	E4 (meV)	E5 (meV)	E6 (meV)	E7 (meV)	E8 (meV)
2	10.145	16.837	40.866	66.002	93.133	141.954	168.827	229.492
4	10.461	17.013	41.591	66.975	92.608	144.818	162.743	229.618
6	10.486	17.028	41.663	67.099	92.529	145.726	160.871	229.727
8	10.488	17.030	41.670	67.113	92.517	145.946	160.385	229.823
10	10.488	17.030	41.671	67.115	92.516	145.995	160.265	229.907

Table S2.8 isolated single QW

x = 0.3					
QW width b (nm)	E1 (meV)	E2 (meV)	E3 (meV)	E4 (meV)	E5 (meV)
15	17	67	146		
20	11	42	93	160	230

10.29322/IJSRP.15.11.2025.p16747

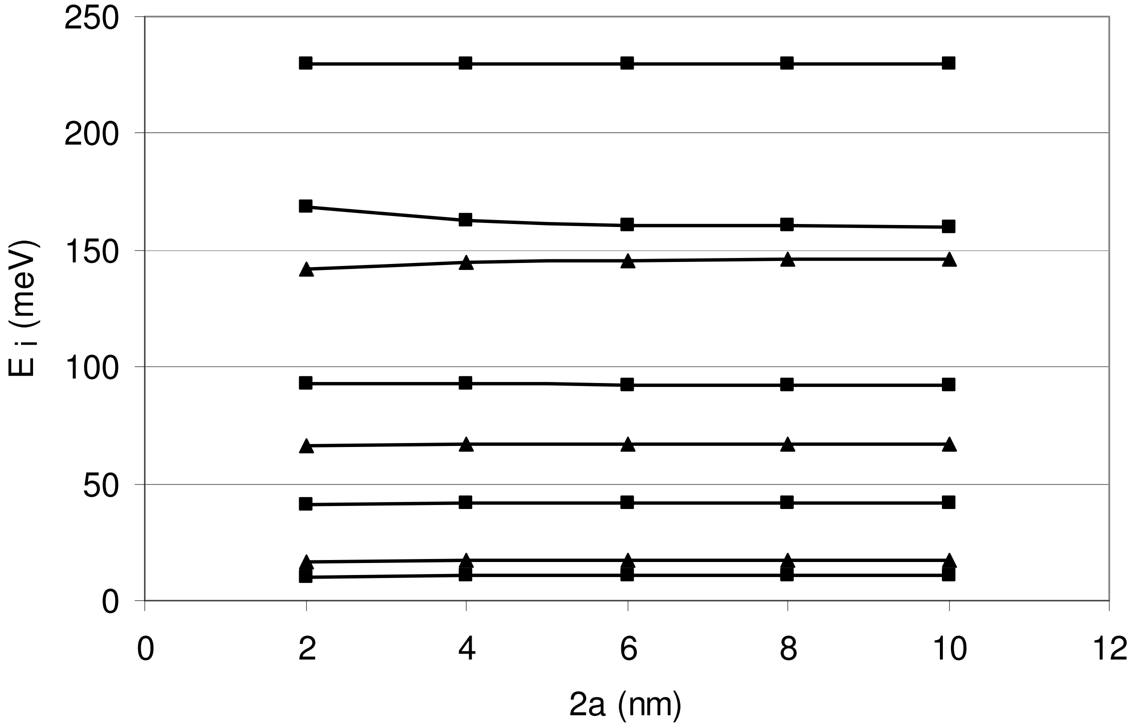

Figure S2.4 Showing data of Table S2.7: quasi-bound energy levels of Coupled Quantum Well for various widths $2a$ of tunnel barrier between the two wells of widths L = 20 nm and r = 15 nm and depth $773x$ = 231.9 meV for Al content x = 0.3 of $Al_xGa_{1-x}As$. Squares originate from isolated left hand QW and triangles originate from isolated right hand QW.

Table S2.9 well widths L = 20 nm, r = 10 nm, Al content of AlGaAs x = 0.3

2a (nm)	E1 (meV)	E2 (meV)	E3 (meV)	E4 (meV)	E5 (meV)	E6 (meV)	E7 (meV)
2	10.247	30.502	42.514	90.179	123.871	165.390	229.821
4	10.469	32.047	41.769	92.164	123.360	161.513	229.920
6	10.487	32.206	41.681	92.466	123.251	160.537	230.006
8	10.488	32.221	41.672	92.509	123.231	160.302	230.080
10	10.488	32.223	41.671	92.515	123.227	160.245	230.144

Table S2.10 isolated single QW

x = 0.3					
QW width b (nm)	E1 (meV)	E2 (meV)	E3 (meV)	E4 (meV)	E5 (meV)
10	32	124			
20	11	42	93	160	230

10.29322/IJSRP.15.11.2025.p16747

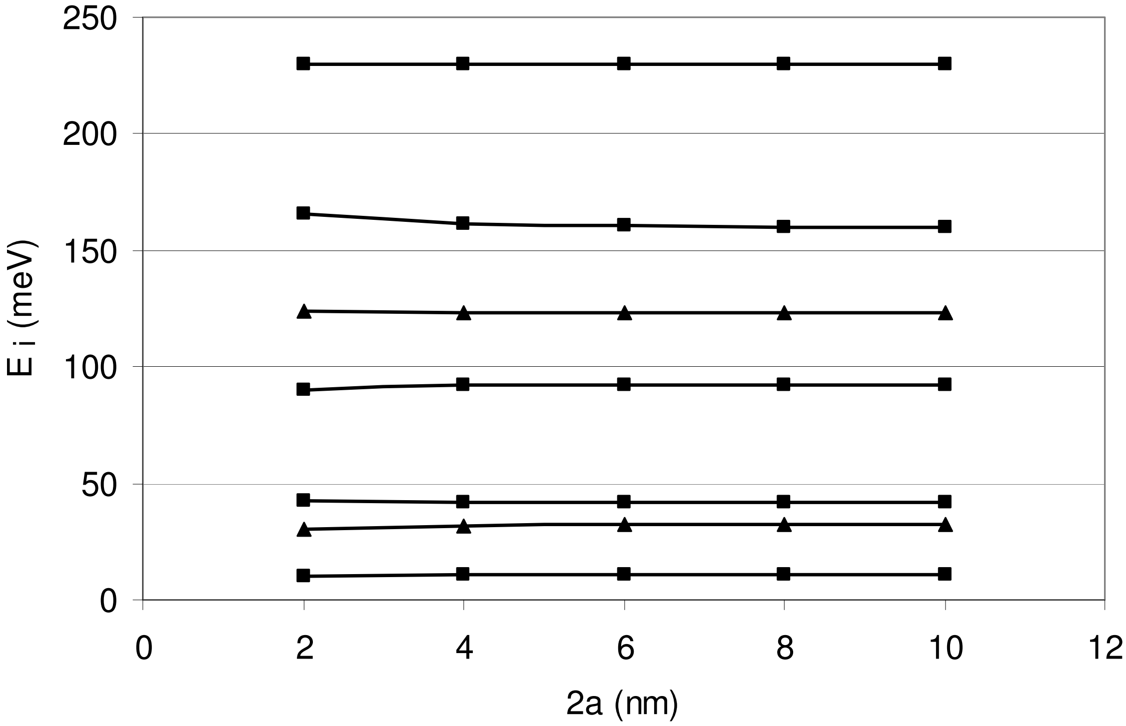

Figure S2.5 Showing data of Table S2.9: quasi-bound energy levels of Coupled Quantum Well for various widths $2a$ of tunnel barrier between the two wells of widths $L = 20$ nm and $r = 10$ nm and depth $773x = 231.9$ meV for Al content $x = 0.3$ of $Al_xGa_{1-x}As$. Squares originate from isolated left hand QW and triangles originate from isolated right hand QW.

10.29322/IJSRP.15.11.2025.p16747

Table S2.11 well widths L = 20 nm, r = 5 nm, Al content of AlGaAs x = 0.3

2a (nm)	E1 (meV)	E2 (meV)	E3 (meV)	E4 (meV)	E5 (meV)	E6 (meV)
2	10.321	40.415	74.928	98.778	162.765	230.174
4	10.475	41.549	79.561	93.755	160.838	230.232
6	10.487	41.659	80.473	92.701	160.374	230.281
8	10.488	41.670	80.601	92.541	160.262	230.323
10	10.488	41.671	80.618	92.519	160.235	230.358

Table S2.12 isolated single QW

x = 0.3					
QW width b (nm)	E1 (meV)	E2 (meV)	E3 (meV)	E4 (meV)	E5 (meV)
5	81				
20	11	42	93	160	230

10.29322/IJSRP.15.11.2025.p16747

Energy spectrum of GaAs-AlGaAs Coupled Quantum Well

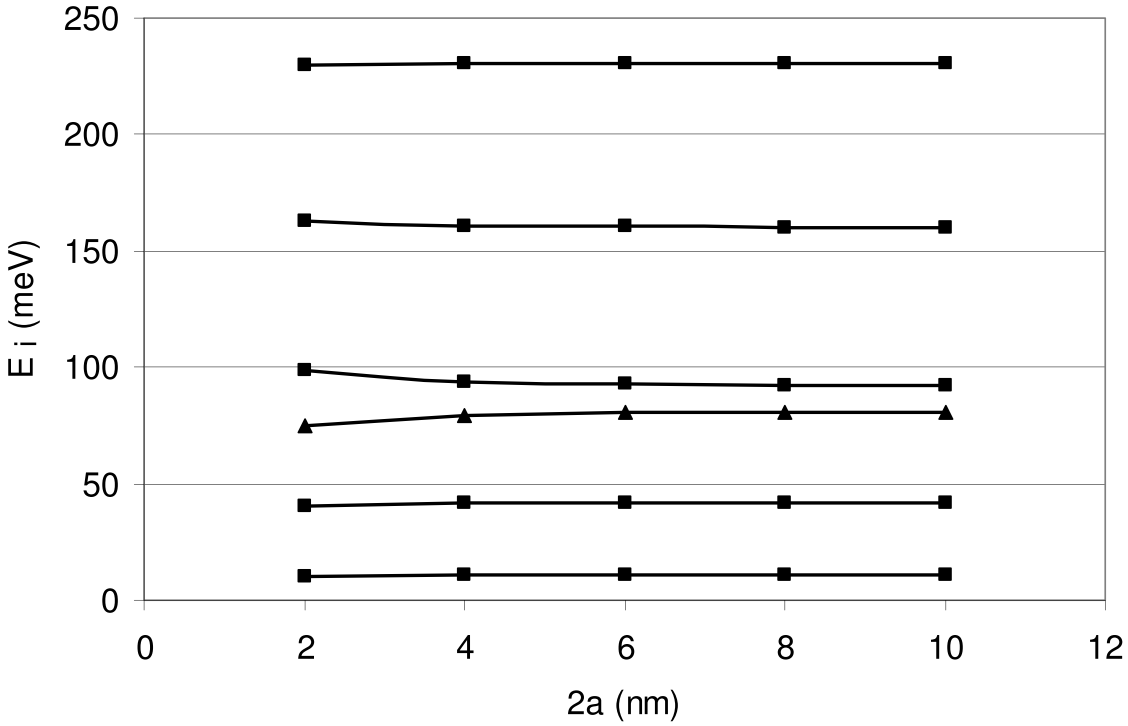

Figure S2.6 Showing data of Table S2.11: quasi-bound energy levels of Coupled Quantum Well for various widths 2*a* of tunnel barrier between the two wells of widths $L = 20$ nm and $r = 5$ nm and depth $773x = 231.9$ meV for Al content $x = 0.3$ of $Al_xGa_{1-x}As$. Squares originate from isolated left hand QW and triangles originate from isolated right hand QW.

10.29322/IJSRP.15.11.2025.p16747

Table S2.13 well widths L = 20 nm, r = 15 nm, Al content of AlGaAs x = 0.2

2a (nm)	E1 (meV)	E2 (meV)	E3 (meV)	E4 (meV)	E5 (meV)	E6 (meV)	E7 (meV)
2	9.219	15.546	37.785	60.498	87.346	128.122	153.31
4	9.781	15.707	38.783	61.143	86.028	128.394	148.282
6	9.852	15.731	38.957	61.295	85.657	128.544	145.403
8	9.862	15.734	38.985	61.326	85.561	128.618	143.945
10	9.863	15.734	38.990	61.332	85.538	128.651	143.201

Table S2.14 isolated single QW

x = 0.2				
QW width b (nm)	E1 (meV)	E2 (meV)	E3 (meV)	E4 (meV)
15	16	61	129	
20	10	39	86	142

10.29322/IJSRP.15.11.2025.p16747

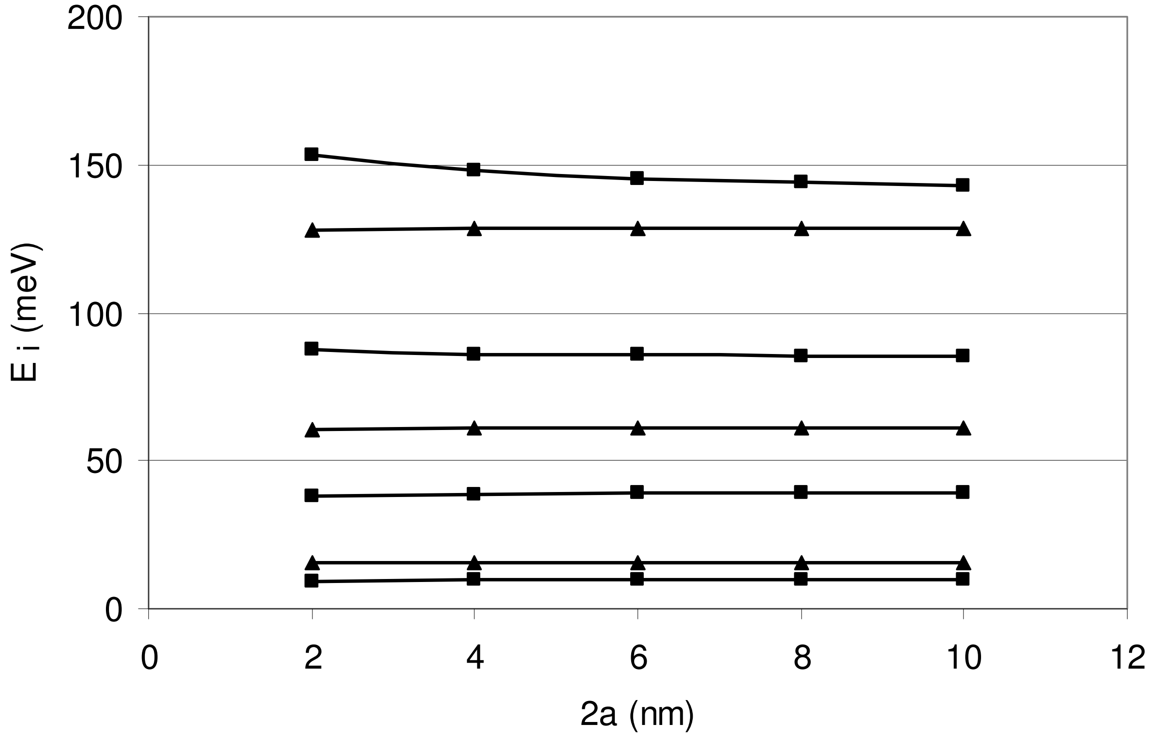

Figure S2.7 Showing data of Table S2.13: quasi-bound energy levels of Coupled Quantum Well for various widths 2*a* of tunnel barrier between the two wells of widths L = 20 nm and r = 15 nm and depth 773x = 154.6 meV for Al content x = 0.2 of $Al_xGa_{1-x}As$. Squares originate from isolated left hand QW and triangles originate from isolated right hand QW.

10.29322/IJSRP.15.11.2025.p16747

Table S2.15 well widths L = 20 nm, r = 10 nm, Al content of AlGaAs x = 0.2

2a (nm)	E1 (meV)	E2 (meV)	E3 (meV)	E4 (meV)	E5 (meV)	E6 (meV)
2	9.428	26.547	40.383	82.280	111.688	150.161
4	9.809	28.426	39.268	84.566	108.466	146.204
6	9.856	28.760	39.039	85.275	107.194	144.285
8	9.862	28.813	38.999	85.465	106.769	143.358
10	9.863	28.821	38.993	85.514	106.635	142.891

Table S2.16 isolated single QW

x = 0.2				
QW width b (nm)	E1 (meV)	E2 (meV)	E3 (meV)	E4 (meV)
10	29	107		
20	10	39	86	142

10.29322/IJSRP.15.11.2025.p16747

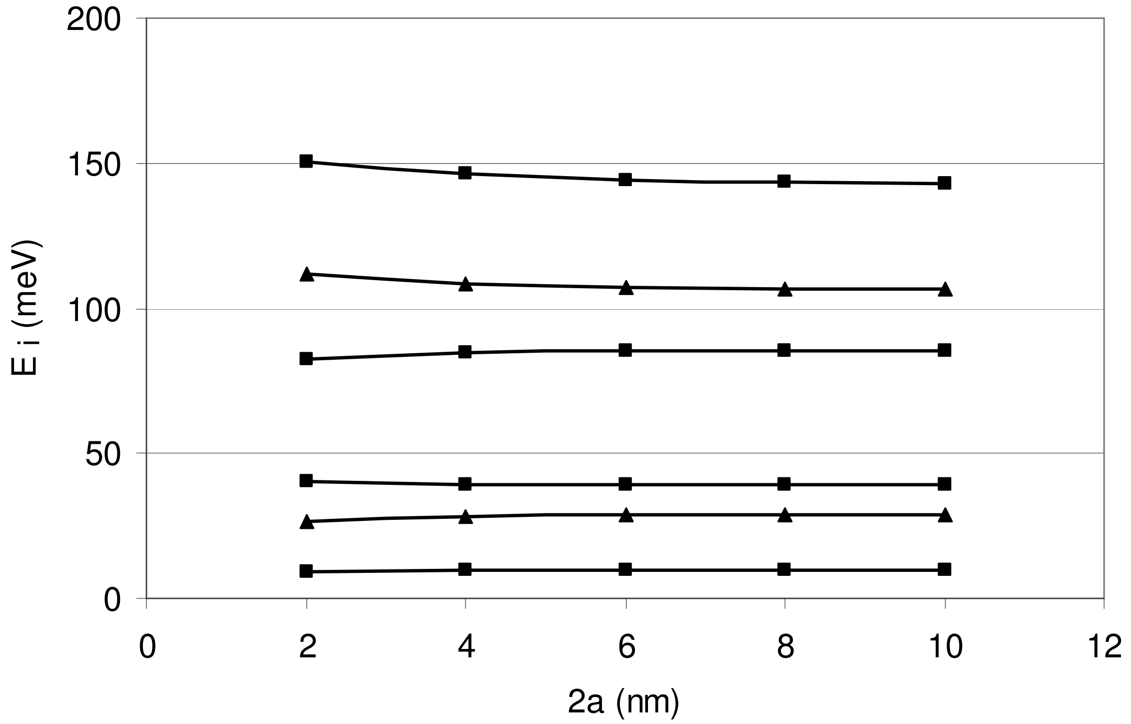

Figure S2.8 Showing data of Table S2.15: quasi-bound energy levels of Coupled Quantum Well for various widths $2a$ of tunnel barrier between the two wells of widths L = 20 nm and r = 10 nm and depth $773x$ = 154.6 meV for Al content x = 0.2 of $Al_xGa_{1-x}As$. Squares originate from isolated left hand QW and triangles originate from isolated right hand QW.

10.29322/IJSRP.15.11.2025.p16747

Table S2.17 well widths L = 20 nm, r = 5 nm, Al content of AlGaAs x = 0.2

2a (nm)	E1 (meV)	E2 (meV)	E3 (meV)	E4 (meV)	E5 (meV)
2	9.578	36.671	63.571	92.573	146.857
4	9.827	38.599	65.772	87.590	144.615
6	9.858	38.926	66.429	86.062	143.523
8	9.863	38.980	66.581	85.663	142.976
10	9.863	38.989	66.613	85.563	142.693

Table S2.18 isolated single QW

x = 0.2				
QW width b (nm)	E1 (meV)	E2 (meV)	E3 (meV)	E4 (meV)
5	67			
20	10	39	86	142

10.29322/IJSRP.15.11.2025.p16747

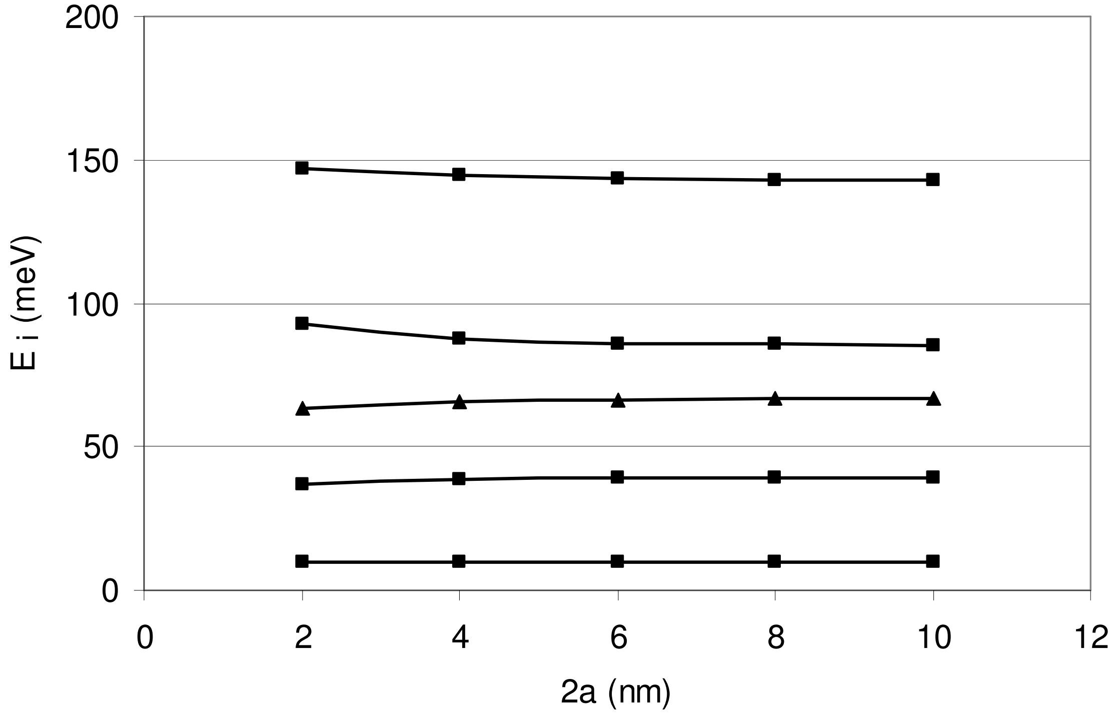

Figure S2.9 Showing data of Table S2.17: quasi-bound energy levels of Coupled Quantum Well for various widths $2a$ of tunnel barrier between the two wells of widths L = 20 nm and r = 5 nm and depth $773x$ = 154.6 meV for Al content x = 0.2 of $Al_xGa_{1-x}As$. Squares originate from isolated left hand QW and triangles originate from isolated right hand QW.

Table S2.19 well widths L = 20 nm, r = 15 nm, Al content of AlGaAs x = 0.1

2a (nm)	E1 (meV)	E2 (meV)	E3 (meV)	E4 (meV)	E5 (meV)
2	7.267	13.423	32.103	51.252	73.759
4	8.276	13.310	32.963	50.392	71.810
6	8.538	13.272	33.297	49.950	70.605
8	8.604	13.261	33.414	49.751	69.905
10	8.621	13.258	33.454	49.666	69.502

Table S2.20 isolated single QW

x = 0.1			
QW width b (nm)	E1 (meV)	E2 (meV)	E3 (meV)
15	13	50	
20	9	33	69

10.29322/IJSRP.15.11.2025.p16747

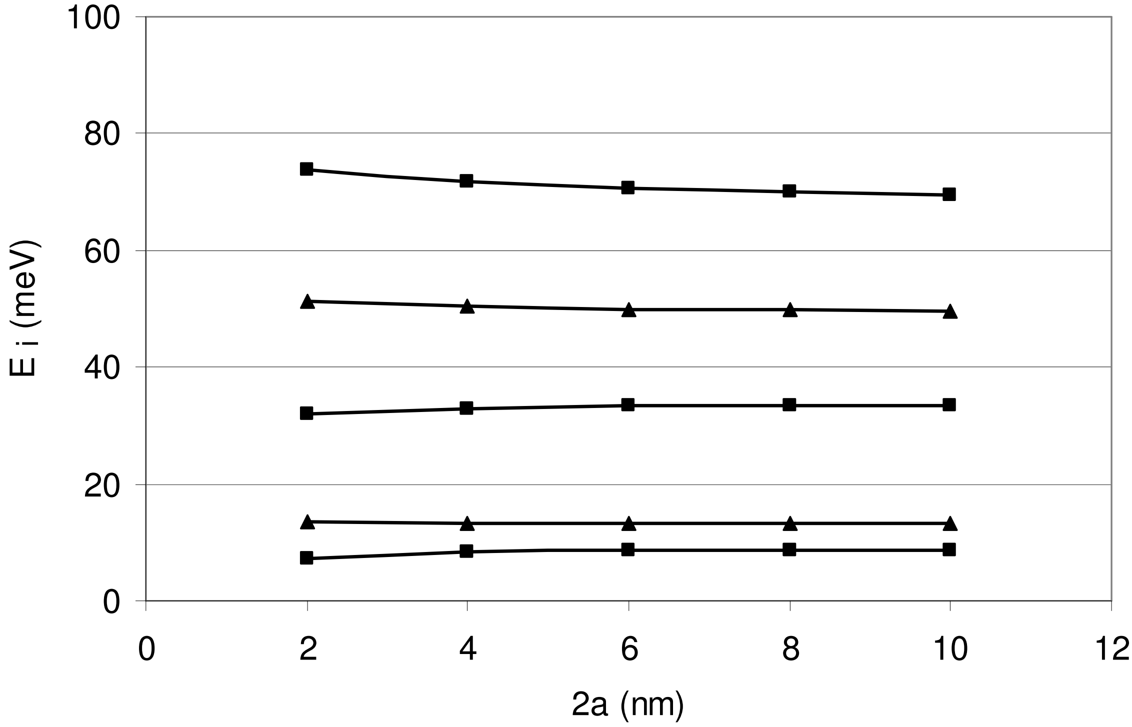

Figure S2.10 Showing data of Table S2.19: quasi-bound energy levels of Coupled Quantum Well for various widths 2*a* of tunnel barrier between the two wells of widths L = 20 nm and r = 15 nm and depth 773x = 77.3 meV for Al content x = 0.1 of $Al_xGa_{1-x}As$. Squares originate from isolated left hand QW and triangles originate from isolated right hand QW.

10.29322/IJSRP.15.11.2025.p16747

Energy spectrum of GaAs-AlGaAs Coupled Quantum Well

Table S2.21 well widths L = 20 nm, r = 10 nm, Al content of AlGaAs x = 0.1

2a (nm)	E1 (meV)	E2 (meV)	E3 (meV)	E4 (meV)	E5 (meV)
2	7.722	20.477	36.048	66.806	
4	8.410	21.926	34.475	67.413	
6	8.573	22.464	33.825	67.867	
8	8.613	22.635	33.592	68.199	76.597
10	8.623	22.687	33.513	68.436	75.739

Table S2.22 isolated single QW

x = 0.1			
QW width b (nm)	E1 (meV)	E2 (meV)	E3 (meV)
10	23	73	
20	9	33	69

10.29322/IJSRP.15.11.2025.p16747

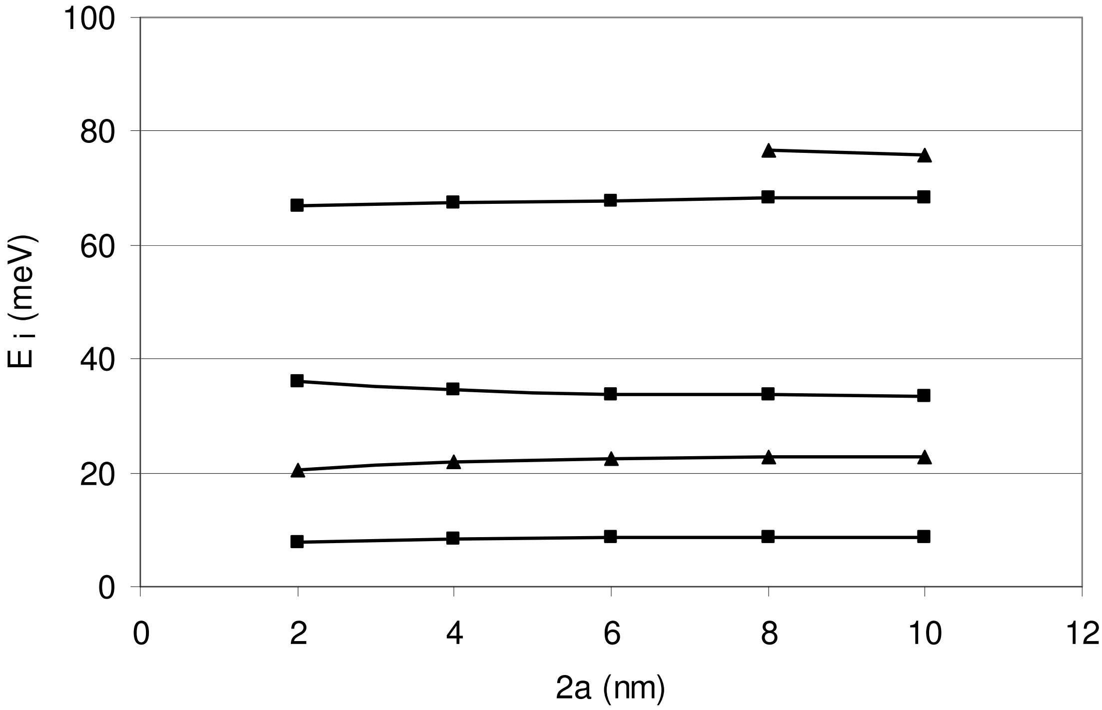

Figure S2.11 Showing data of Table S2.21: quasi-bound energy levels of Coupled Quantum Well for various widths 2*a* of tunnel barrier between the two wells of widths L = 20 nm and r = 10 nm and depth 773x = 77.3 meV for Al content x = 0.1 of $Al_xGa_{1-x}As$. Squares originate from isolated left hand QW and triangles originate from isolated right hand QW.

10.29322/IJSRP.15.11.2025.p16747

Table S2.23 well widths L = 20 nm, r = 5 nm, Al content of AlGaAs x = 0.1

2a (nm)	E1 (meV)	E2 (meV)	E3 (meV)	E4 (meV)
2	8.085	29.051	49.037	75.819
4	8.497	31.685	47.046	72.982
6	8.594	32.815	45.905	71.214
8	8.618	33.246	45.379	70.231
10	8.624	33.397	45.161	69.682

Table S2.24 isolated single QW

x = 0.1			
QW width b (nm)	E1 (meV)	E2 (meV)	E3 (meV)
5	45		
20	9	33	69

10.29322/IJSRP.15.11.2025.p16747

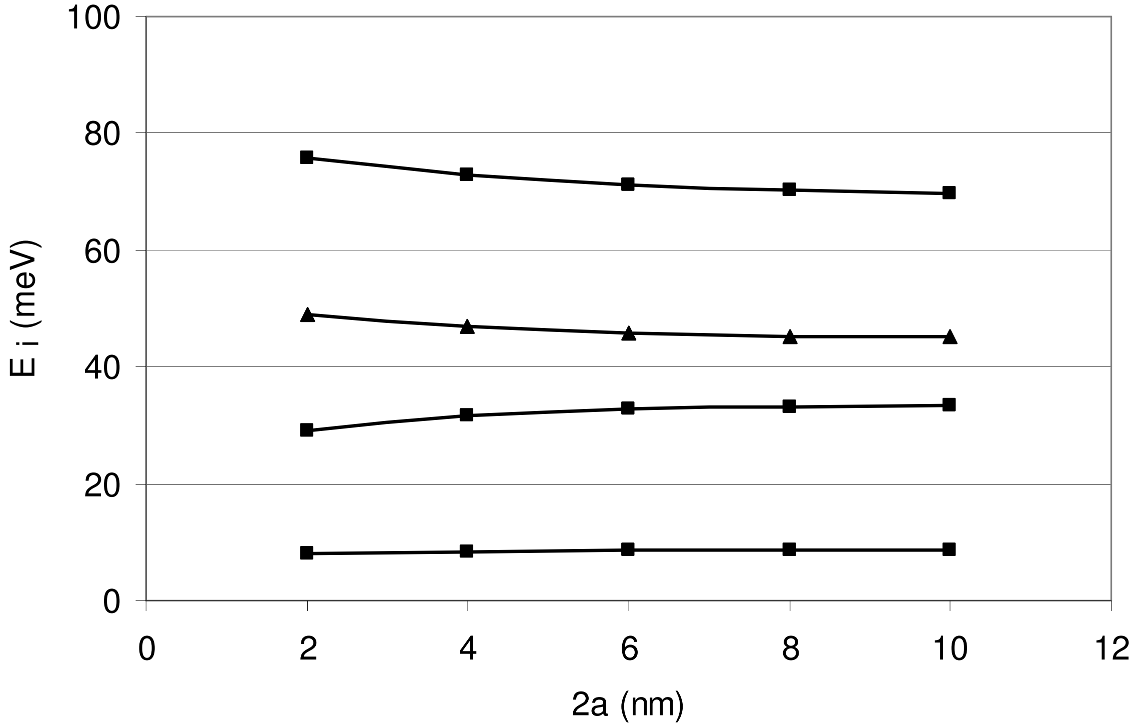

Figure S2.12 Showing data of Table S2.23: quasi-bound energy levels of Coupled Quantum Well for various widths 2*a* of tunnel barrier between the two wells of widths $L = 20$ nm and $r = 5$ nm and depth $773x = 77.3$ meV for Al content $x = 0.1$ of $Al_xGa_{1-x}As$. Squares originate from isolated left hand QW and triangles originate from isolated right hand QW.

10.29322/IJSRP.15.11.2025.p16747

Table S2.25 for isolated QWs

x = 0.3			
QW width b (nm)	E1 (meV)	E2 (meV)	E3 (meV)
5.9	67	218	
15	17	67	146

Table S2.26 well widths L = 15 nm, r = 5.9 nm, Al content of AlGaAs x = 0.3

2a (nm)	E1 (meV)	E2 (meV)	E3 (meV)	E4 (meV)	E5 (meV)
2	16.604	57.416	75.135	146.882	219.659
4	16.994	63.626	69.787	146.200	218.781
6	17.027	65.618	67.843	146.049	218.221
8	17.030	66.206	67.255	146.017	217.900
10	17.030	66.326	67.134	146.010	217.726

10.29322/IJSRP.15.11.2025.p16747

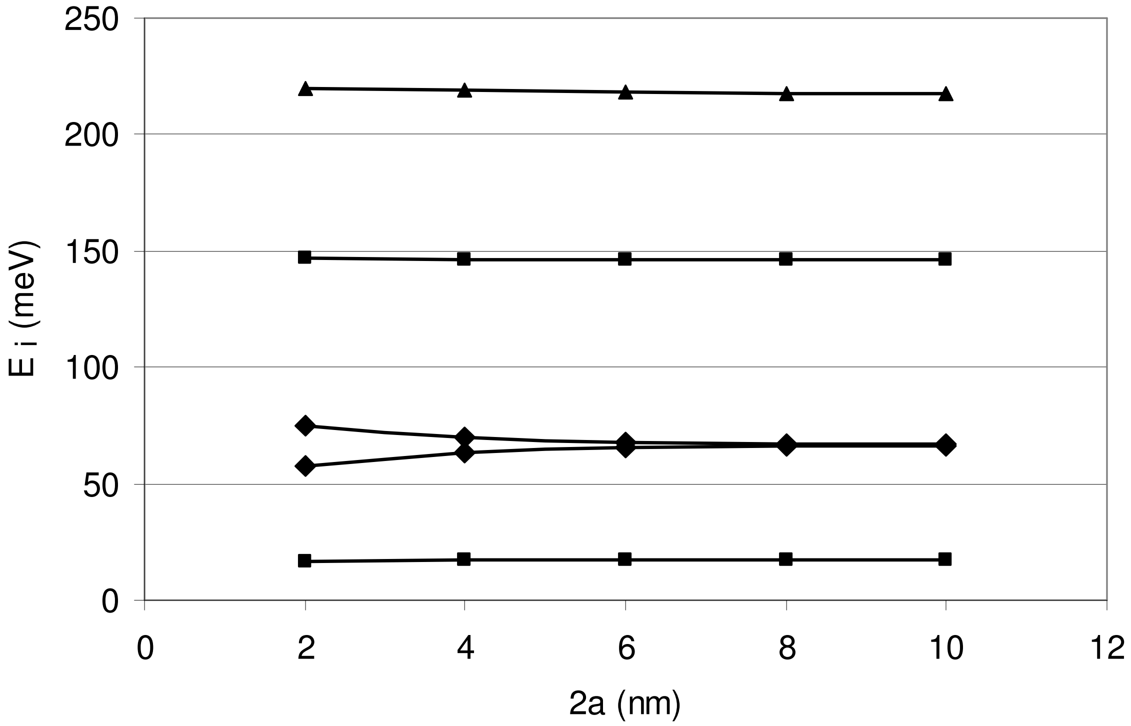

Figure S2.13 Showing data of Table S2.26: quasi-bound energy levels of Coupled Quantum Well for various widths 2*a* of tunnel barrier between the two wells of widths L = 15 nm and r = 5.9 nm and depth 773x = 231.9 meV for Al content x = 0.3 of $Al_xGa_{1-x}As$. Squares originate from isolated left hand QW and triangles originate from isolated right hand QW. Data in diamonds show energy *doublets* corresponding to equal energy levels of the two isolated QWs at 67 meV; see Table S2.25.

10.29322/IJSRP.15.11.2025.p16747

Table S2.27 for isolated QWs

x = 0.3		
QW width b (nm)	E1 (meV)	E2 (meV)
3.24	124	
10	32	124

Table S2.28 well widths L = 10 nm, r = 3.24 nm, Al content of AlGaAs x = 0.3

2a (nm)	E1 (meV)	E2 (meV)	E3 (meV)
2	31.296	104.855	146.82
4	32.137	115.294	132.758
6	32.215	119.836	127.084
8	32.222	121.809	124.829
10	32.223	122.655	123.919

10.29322/IJSRP.15.11.2025.p16747

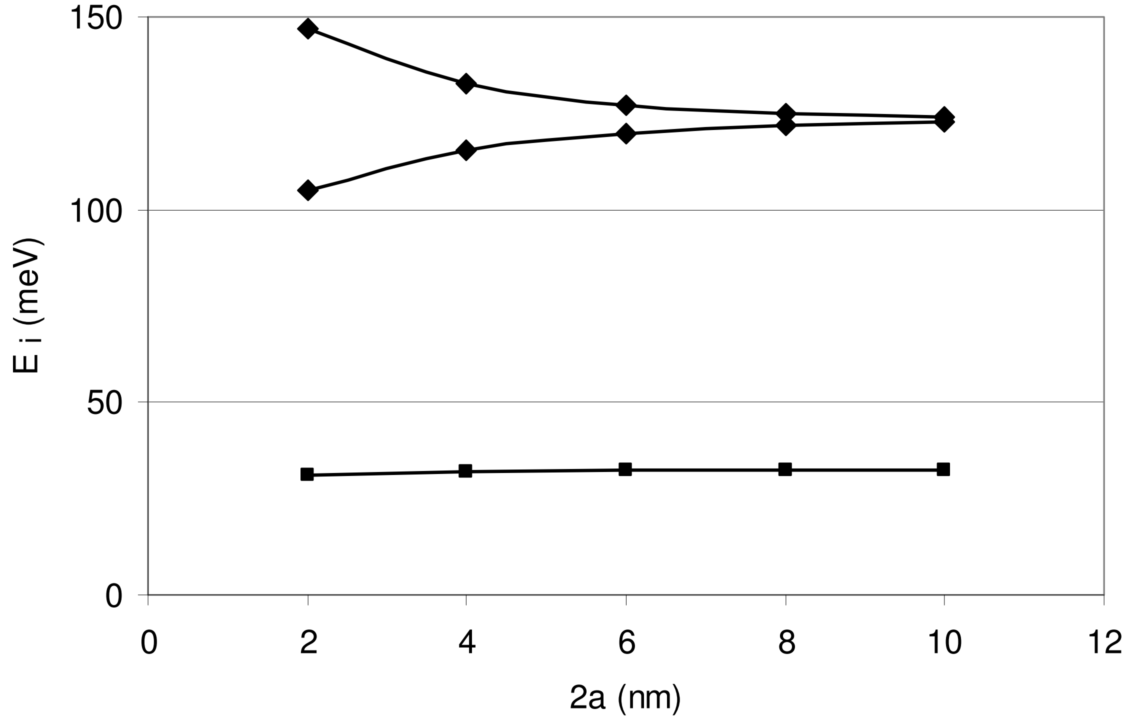

Figure S2.14 Showing data of Table S2.28: quasi-bound energy levels of Coupled Quantum Well for various widths $2a$ of tunnel barrier between the two wells of widths L = 10 nm and r = 3.24 nm and depth $773x$ = 231.9 meV for Al content x = 0.3 of $Al_xGa_{1-x}As$. Squares originate from isolated left hand QW. Data in diamonds show energy *doublets* corresponding to equal energy levels of the two isolated QWs at 124 meV; see Table S2.27.

10.29322/IJSRP.15.11.2025.p16747

Table S2.29 for isolated QWs

x = 0.2				
QW width b (nm)	E1 (meV)	E2 (meV)	E3 (meV)	E4 (meV)
3.8	86			
20	10	39	86	142

Table S2.30 well widths L = 20 nm, r = 3.8 nm, Al content of AlGaAs x = 0.2

2a (nm)	E1 (meV)	E2 (meV)	E3 (meV)	E4 (meV)	E5 (meV)
2	9.622	37.343	73.426	100.711	150.401
4	9.832	38.720	79.066	93.023	146.199
6	9.859	38.946	82.104	89.061	144.256
8	9.863	38.984	83.686	87.156	143.337
10	9.863	38.990	84.492	86.247	142.879

10.29322/IJSRP.15.11.2025.p16747

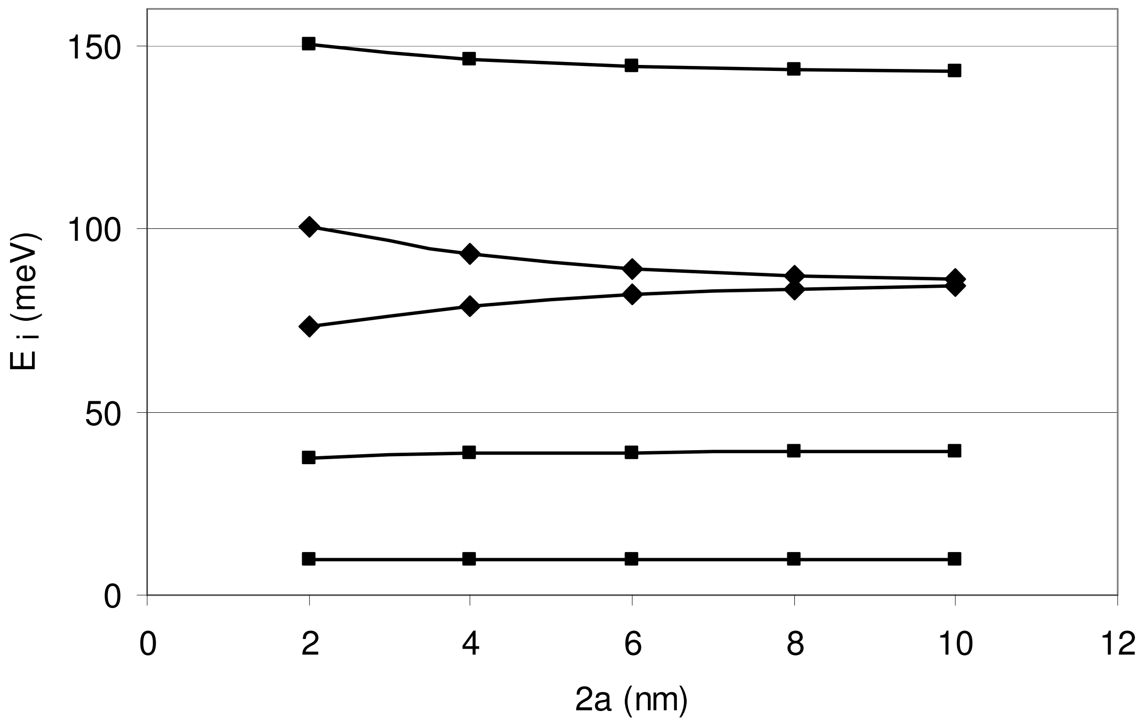

Figure S2.15 Showing data of Table S2.30: quasi-bound energy levels of Coupled Quantum Well for various widths $2a$ of tunnel barrier between the two wells of widths L = 20 nm and r = 3.8 nm and depth $773x$ = 154.6 meV for Al content x = 0.2 of $Al_xGa_{1-x}As$. Squares originate from isolated left hand QW. Data in diamonds show energy *doublets* corresponding to equal energy levels of the two isolated QWs at 86 meV; see Table S2.29.

10.29322/IJSRP.15.11.2025.p16747

Table S2.31 For 2a = 2 nm, well widths L = 20 nm, r = 15 nm

x	E1 (meV)	E2 (meV)	E3 (meV)	E4 (meV)	E5 (meV)	E6 (meV)	E7 (meV)	E8 (meV)	E9 (meV)
0.1	7.267	13.423	32.103	51.252	73.759				
0.2	9.219	15.546	37.785	60.498	87.346	128.122	153.31		
0.3	10.145	16.837	40.866	66.002	93.133	141.954	168.827	229.492	
0.4	10.685	17.719	42.818	69.828	96.884	151.400	175.283	250.100	281.279

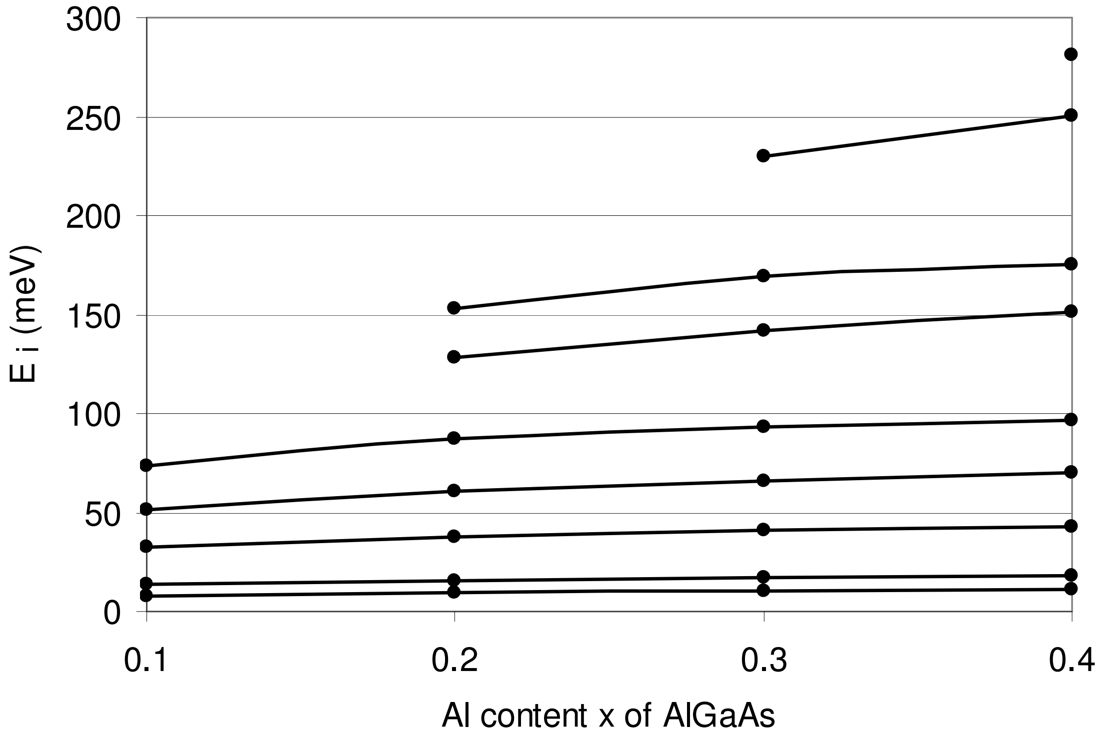

Figure S2.16 Showing data of Table S2.31: quasi-bound energy levels of Coupled Quantum Well for various depths 773*x* meV corresponding to various Al contents *x* of $Al_xGa_{1-x}As$. For QW widths L = 20 nm and r = 15 nm and tunnel barrier width 2a = 2 nm.

10.29322/IJSRP.15.11.2025.p16747

Table S2.32 For 2a = 10 nm, well widths L = 20 nm, r = 15 nm

x	E1 (meV)	E2 (meV)	E3 (meV)	E4 (meV)	E5 (meV)	E6 (meV)	E7 (meV)	E8 (meV)	E9 (meV)
0.1	8.621	13.258	33.454	49.666	69.502				
0.2	9.863	15.734	38.990	61.332	85.538	128.651	143.201		
0.3	10.488	17.030	41.671	67.115	92.516	145.995	160.265	229.907	
0.4	10.887	17.871	43.351	70.7718	96.703	155.926	169.316	256.397	264.333

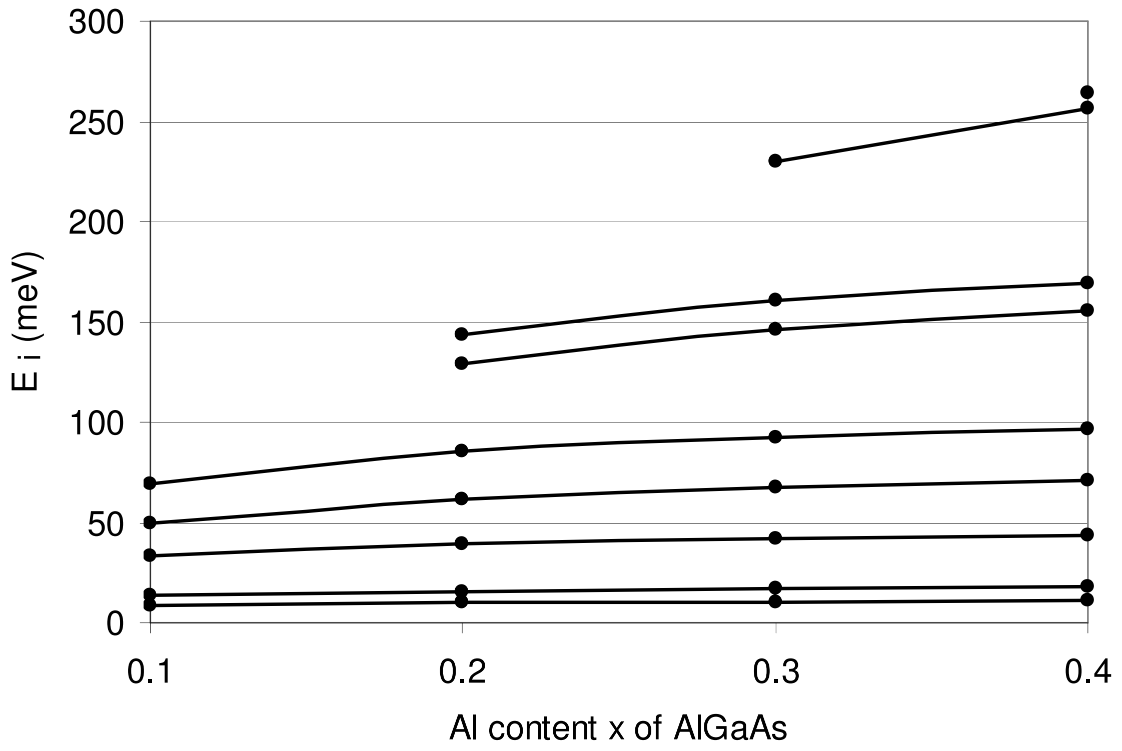

Figure S2.17 Showing data of Table S2.32: quasi-bound energy levels of Coupled Quantum Well for various depths 773x meV corresponding to various Al contents x of $Al_xGa_{1-x}As$. For QW widths L = 20 nm and r = 15 nm and tunnel barrier width 2a = 10 nm.

10.29322/IJSRP.15.11.2025.p16747

Energy spectrum of GaAs-AlGaAs Coupled Quantum Well

Table S2.33 For 2a = 2 nm, well widths L = 20 nm, r = 10 nm

x	E1 (meV)	E2 (meV)	E3 (meV)	E4 (meV)	E5 (meV)	E6 (meV)	E7 (meV)	E8 (meV)
0.1	7.722	20.477	36.048	66.806				
0.2	9.428	26.547	40.383	82.280	111.688	150.161		
0.3	10.247	30.502	42.514	90.179	123.871	165.390	229.821	
0.4	10.741	33.258	43.896	95.139	132.890	172.592	252.442	292.361

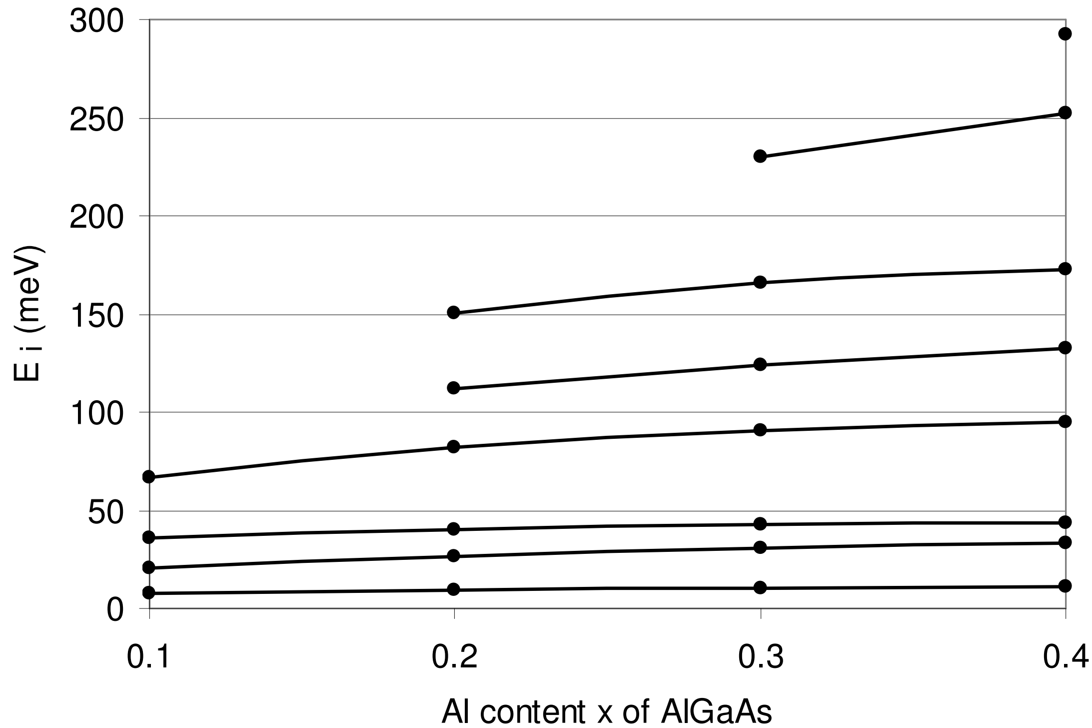

Figure S2.18 Showing data of Table S2.33: quasi-bound energy levels of Coupled Quantum Well for various depths 773*x* meV corresponding to various Al contents *x* of $Al_xGa_{1-x}As$. For QW widths L = 20 nm and r = 10 nm and tunnel barrier width $2a$ = 2 nm.

Table S2.34 For 2a = 10 nm, well widths L = 20 nm, r = 10 nm

x	E1 (meV)	E2 (meV)	E3 (meV)	E4 (meV)	E5 (meV)	E6 (meV)	E7 (meV)	E8 (meV)
0.1	8.623	22.687	33.513	68.436	75.739			
0.2	9.863	28.821	38.993	85.514	106.635	142.891		
0.3	10.488	32.223	41.671	92.515	123.227	160.245	230.144	
0.4	10.887	34.505	43.351	96.703	133.896	169.314	256.483	276.004

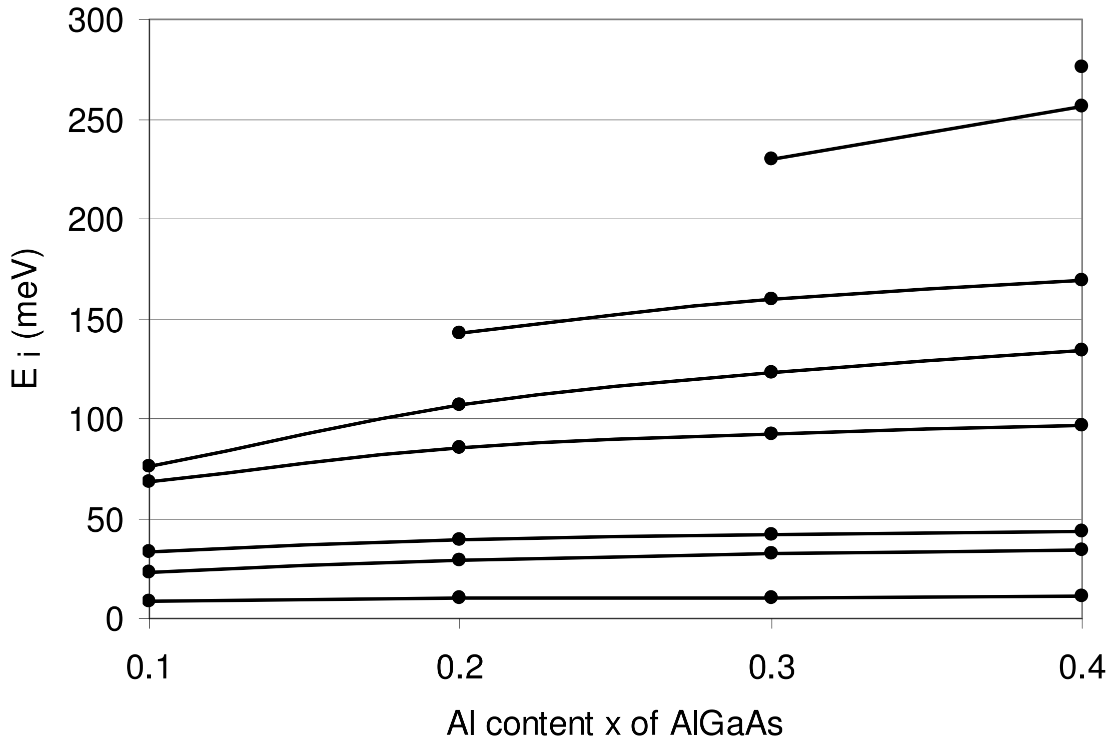

Figure S2.19 Showing data of Table S2.34: quasi-bound energy levels of Coupled Quantum Well for various depths 773x meV corresponding to various Al contents x of $Al_xGa_{1-x}As$. For QW widths L = 20 nm and r = 10 nm and tunnel barrier width 2a = 10 nm.

Table S2.35 For 2a = 2 nm, well widths L = 20 nm, r = 5 nm

x	E1 (meV)	E2 (meV)	E3 (meV)	E4 (meV)	E5 (meV)	E6 (meV)	E7 (meV)
0.1	8.085	29.051	49.037	75.819			
0.2	9.578	36.671	63.571	92.573	146.857		
0.3	10.321	40.415	74.928	98.778	162.765	230.174	
0.4	10.781	42.607	84.057	102.804	170.798	254.606	307.789

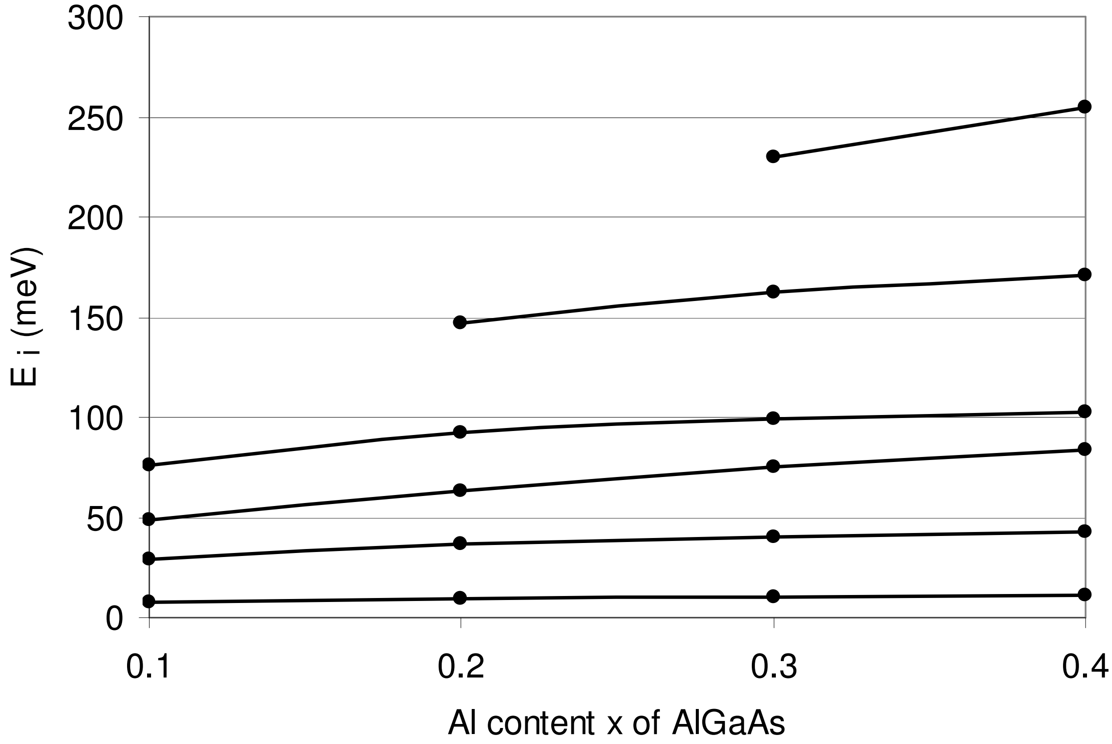

Figure S2.20 Showing data of Table S2.35: quasi-bound energy levels of Coupled Quantum Well for various depths 773*x* meV corresponding to various Al contents *x* of $Al_xGa_{1-x}As$. For QW widths L = 20 nm and r = 5 nm and tunnel barrier width $2a$ = 2 nm.

10.29322/IJSRP.15.11.2025.p16747

Energy spectrum of GaAs-AlGaAs Coupled Quantum Well

Table S2.36 For 2a = 10 nm, well widths L = 20 nm, r = 5 nm

x	E1 (meV)	E2 (meV)	E3 (meV)	E4 (meV)	E5 (meV)	E6 (meV)	E7 (meV)
0.1	8.624	33.397	45.161	69.682			
0.2	9.863	38.989	66.613	85.563	142.693		
0.3	10.488	41.671	80.618	92.519	160.235	230.358	
0.4	10.887	43.351	90.831	96.704	169.313	256.514	294.741

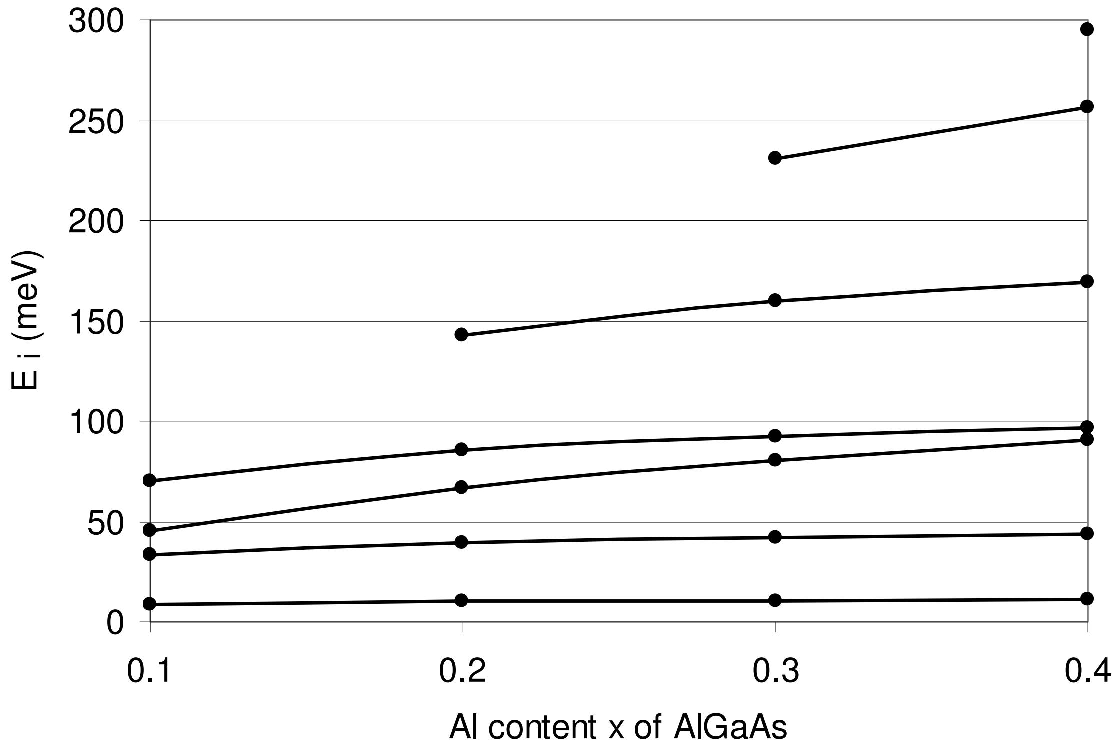

Figure S2.21 Showing data of Table S2.36: quasi-bound energy levels of Coupled Quantum Well for various depths 773*x* meV corresponding to various Al contents *x* of $Al_xGa_{1-x}As$. For QW widths $L = 20$ nm and $r = 5$ nm and tunnel barrier width $2a = 10$ nm.

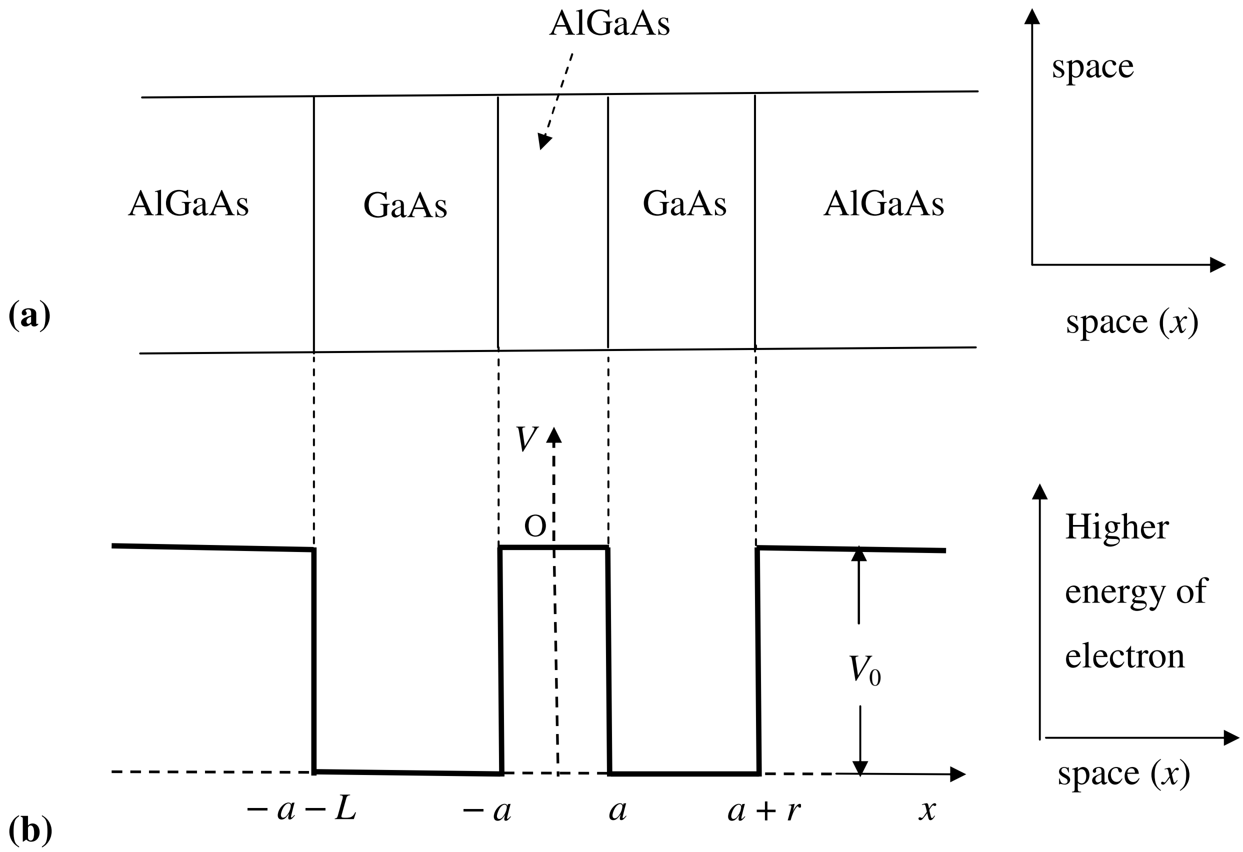

Figure S2.22 (a) Material structure (b) band model of GaAs-AlGaAs Coupled Quantum Well. O is origin (0, 0) of the coordinate system. Potential energy V is $-V_0$ in the Quantum Wells because of the choice of origin. QW widths L and r are different. This is to help describe consequences of taking origin O at the top rather than bottom of the band model.

If origin O($x = 0$, $V(x) = 0$) of the potential energy profile is taken at the top of the QW as in Figure S2.22, allowed values of E come out as negative numbers and are called energy of bound states of nanostructure. In our calculations, we have taken the origin at the bottom of the QWs and we are exploring the energy range $0 < E < V_0$. As such allowed values of E that have come out are positive and are allowed values of kinetic energy of an electron inside the QWs for motion along x direction. $E < V_0$ still ensures that electrons residing in the CQW are classically not allowed to go out of the CQW and are bound to the CQW.